Global and Robust Attitude Control of a Launch Vehicle in Exoatmospheric Flight[1]

Fabio Celani

School of Aerospace Engineering
Sapienza University of Rome
Via Salaria 851, 00138 Roma, Italy
fabio.celani@uniroma1.it
http://fabiocelani.site.uniroma1.it/

Abstract

The goal of this research is to design global and robust attitude control systems for launch vehicles in exoatmospheric flight. An attitude control system is global when it guarantees that the vehicle converges to the desired attitude regardless of its initial condition. Global controllers are important because when large angle maneuvers must be performed, it is simpler to use a single global controller than several local controllers patched together. In addition, the designed autopilots must be robust with respect to uncertainties in the parameters of the vehicle, which means that global convergence must be achieved despite of those uncertainties. Two designs are carried out. In the first one possible delays introduced by the actuator are neglected. The design is performed by using a Lyapunov approach, and the obtained autopilot is a standard proportional-derivative controller. In the second one, the effects of the actuator are considered. Then the design is based on robust backstepping which leads to a memory-less nonlinear feedback of attitude, attitude-rate, and of the engine deflection angle. Both autopilots are validated in a case study.

Keywords: attitude control, launch vehicle, nonlinear control systems, robust global stabilization

[1]DOI of the formal publication:10.1016/j.ast.2017.12.016

1. Introduction

Designing an autopilot for a launch vehicle is a challenging task due to its nonlinear and time-varying properties (see [1]). Several attitude controllers have been proposed over the years. For example, baseline Proportional-Derivative (PD) controllers are designed in [1, Section 5.3]. An intelligent adaptive autopilot is presented in [2]. Paper [3] proposes a design based on adaptive predictive control. Model reference adaptive control is employed in [4] to design PD and Proportional-Integral-Derivative (PID) autopilots. In addition, in the last decades many designs based on modern robust control have been proposed. For instance, H_∞ control is used in [5, 6, 7], whereas μ-synthesis in employed in [8]. In paper [9] a method known as Wave-Based Control is applied to designing an autopilot capable of compensating for the effects of fuel-sloshing. All the above design methods are based on linearized models of the vehicle. As a results, those methods assure only local convergence. Then, from an analytical standpoint, the attitude is guaranteed to converge to the desired one only if the initial condition of the vehicle is sufficiently close to that attitude.

The goal of the present work is to address the latter issue by designing autopilots that achieve global convergence so that it is analytically assured that the desired attitude is reached starting from any initial condition. Global autopilots are particularly convenient when a launch vehicle must perform large angle maneuvers. In fact, in such a scenario, one can use a single global attitude controller instead of several local controllers patched together through some scheduling strategy. The latter fact simplifies the actual implementation of the autopilot on the on board computer. In addition, the designed autopilots must be robust with respect to uncertainties in the parameters of the vehicle, which means that global convergence must be achieved despite of those uncertainties. The latter uncertainties are a consequence of slow variations of some parameters during flight and of limited accuracy in the determination of their values.

A global autopilot has been recently presented in [10]. The latter controller has been designed for the atmospheric flight of a launch vehicle modeled as a rigid body. In this paper global autopilot design is carried out for an upper stage of a launch vehicle flying above atmosphere. Global attitude controllers are more useful during the exoatmospheric flight than during the atmospheric one. This is a consequence of the fact that they are especially suited for performing large angle maneuvers which can occur only above the atmosphere. In fact, during the atmospheric flight launch vehicles cannot perform those maneuvers because of constraints imposed by aerodynamic loads. In particular, large angle maneuvers often occur at the beginning of the exoatmospheric flight for the following reason. During atmospheric flight launch vehicles are mostly guided in gravity turn mode to reduce the aerodynamic load [11, 12]. Thus, at the beginning of the exoatmospheric flight, it often happens that the vehicle is distant from the desired trajectory, and consequently large angle attitude maneuvers are necessary for having it converge to that trajectory. Additional differences of this research with respect to [10] are as follows. The designs in this study take into account the limit values for the engine deflection angle, and one of the designs considers the effects of the electrohydraulic actuator on the vehicle dynamics. Both latter aspects have been neglected in [10].

In this work a motion occurring on a vertical plane is considered since the flight of most launch vehicles is basically confined to such a plane (see [13, Chapter 4]). As a result, significant attitude maneuvers must occur in the trajectory plane, whereas only minor attitude corrections must be performed off that plane. The launch vehicle is here modeled as a rigid body. In fact, for some upper stages the nonlinear effects due to flexibility, liquid sloshing and engine inertia are not significant. As a matter of fact, flexibility is often negligible for upper stages because of their reduced length and because of the absence of aerodynamic loads. In addition, fuel sloshing effects are negligible for launch vehicles with baffles inside the tanks or in which the tank is divided into several smaller ones. Finally, engine inertia effects are not significant when the mass of the swiveling engine is negligible with respect to the mass of the

main body.

The rest of the paper is organized as follows. In section 2 the model of the launch vehicle is presented. In section 3 a global and robust attitude controller is designed not considering the dynamics of the actuator. As a result, the latter design is effective when the actuator is much faster than the designed autopilot. In section 4 the design is carried out including a simple dynamic model for the actuator. Thus, the latter design is important when the actuator is not substantially faster than the designed controller. Both proposed designs are validated in a case study presented in section 5.

2. Model of the Launch Vehicle

Consider an upper stage of a launch vehicle flying in vertical planar trajectory above the atmospheric level. Thrust vector control is used to control the attitude. The pitch plane dynamics (see Fig. 1) are given by (see Chapter 1 of

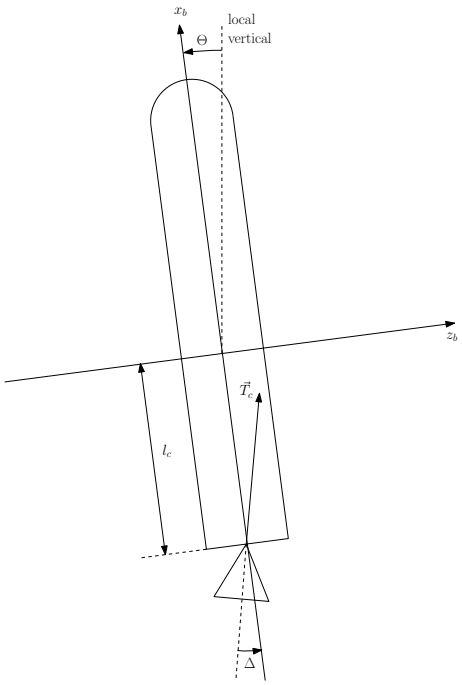

Figure 1: Schematic diagram of launch vehicle.

reference [1])

$$
\begin{aligned}
-mg\cos\Theta + T_c\cos(\mathrm{sat}_{\overline{\Delta}}(\Delta)) &= m(\dot{U} + QW) && (1)\\
-mg\sin\Theta + T_c\sin(\mathrm{sat}_{\overline{\Delta}}(\Delta)) &= m(\dot{W} - QU) && (2)\\
l_c T_c\sin(\mathrm{sat}_{\overline{\Delta}}(\Delta)) &= I\dot{Q} && (3)\\
\dot{\Theta} &= Q && (4)
\end{aligned}
$$

The meaning of the variables and parameters used in the above equations is indicated in Appendix E. Symbol $\mathrm{sat}_{\overline{\Delta}}$ denotes the following saturation function that is introduced to take into account of the limit $0 < \overline{\Delta} < \pi/2$ on the amplitude of the engine deflection angle

$$
\mathrm{sat}_{\overline{\Delta}}(\Delta) \triangleq \begin{cases} -\overline{\Delta} & \text{if } \Delta < -\overline{\Delta} \\ \Delta & \text{if } -\overline{\Delta} \le \Delta \le \overline{\Delta} \\ \overline{\Delta} & \text{if } \Delta > \overline{\Delta}\,. \end{cases} \qquad (5)
$$

In designing the controller, parameters I, l_c, m, and T_c are considered constant but subject to uncertainty due to both their possible slow variations with time, and to limited accuracy in determining their values.

The goal is controlling pitch angle Θ acting on engine deflection angle Δ through a servoactuator. Measures of pitch angle Θ, pitch rate Q, and of the engine deflection angle Δ are considered available to the autopilot.

The electro-hydraulic servoactuator that acts on the engine deflection angle is here modeled by the following first order system (see [1, Section 3.2.3.1])

$$
\dot{\Delta} = -\frac{1}{\tau_a}\Delta + \frac{1}{\tau_a}\Delta_c \qquad (6)
$$

In the above equation Δ_c is the commanded engine deflection angle which represents the control input.

3. Autopilot Design not Including the Dynamics of the Actuator

In this section attitude control design is performed without including model in Eq.(6) for the electro-hydraulic servoactuator. Consequently, the control

input is given directly by Δ. Clearly, the latter simplification is acceptable whenever the actuator is much faster than the resulting autopilot.

Consider only equations (3) and (4) since they are decoupled from equations (1) and (2). They can be rewritten as follows

$$\begin{aligned} \dot{\Theta} &= Q \\ \dot{Q} &= G \sin(\text{sat}_{\overline{\Delta}}(\Delta)) \end{aligned} \tag{7}$$

in which $G = l_c T_c / I$.

Let Θ_c denote the commanded pitch angle. Since attitude commands, which are provided by the guidance system, vary slowly with respect to attitude dynamics, Θ_c is modeled as constant. Consider the following Proportional-Derivative (PD) control law

$$\Delta = k_p(\Theta_c - \Theta) - k_d Q \tag{8}$$

with $k_p > 0$ and $k_d > 0$. Let $\widetilde{\Theta} = \Theta - \Theta_c$; then, the closed-loop system obtained combining Eqs. (7) and (8) writes as follows

$$\begin{aligned} \dot{\widetilde{\Theta}} &= Q \\ \dot{Q} &= -G \sin(\text{sat}_{\overline{\Delta}}(k_p \widetilde{\Theta} + k_d Q)) \end{aligned} \tag{9}$$

The following result holds true.

Theorem 1. *The origin of the closed-loop system in Eq. (9) is globally asymptotically stable.*

Proof. Consider the Lyapunov function

$$V(\widetilde{\Theta}, Q) = k_p Q^2 + 2G \int_0^{-(k_p \widetilde{\Theta} + k_d Q)} \sin(\text{sat}_{\overline{\Delta}}(\Delta)) d\Delta \tag{10}$$

obtained through a simple modification of the Laypunov function considered in [14]. Note that $V(\widetilde{\Theta}, Q) \geq 0$. Moreover $V(\widetilde{\Theta}, Q) = 0$ implies $[\widetilde{\Theta}\ Q]^T = [0\ 0]^T$; consequently, $V(\widetilde{\Theta}, Q)$ is positive definite. In addition, it is immediate to verify that $V(\widetilde{\Theta}, Q)$ is radially unbounded. It is easy to see that the following holds

$$\begin{aligned} \dot{V}(\widetilde{\Theta}, Q) &= 2k_p Q \dot{Q} + 2G \sin(\text{sat}_{\overline{\Delta}}(k_p \widetilde{\Theta} + k_d Q))(k_p \dot{\widetilde{\Theta}} + k_d \dot{Q}) \\ &= -2k_d G^2 \sin^2(\text{sat}_{\overline{\Delta}}(k_p \widetilde{\Theta} + k_d Q)) \end{aligned} \tag{11}$$

Thus, $\dot{V}(\widetilde{\Theta}, Q) \leq 0$, and $\dot{V}(\widetilde{\Theta}, Q) = 0$ implies $k_p\widetilde{\Theta}+k_dQ = 0$. Then, by La Salle's invariance principle (see corollary 4.2 of [15]), it follows that $[\widetilde{\Theta} \;\; Q]^T = [0 \; 0]^T$ is globally asymptotically stable. □

The previous theorem shows that $[\Theta \;\; Q]^T = [\Theta_c \; 0]^T$ is a globally asymptotically stable equilibrium for system in Eq. (7) controlled by feedback in Eq. (8). Consequently, Θ converges to Θ_c starting from any initial condition $[\Theta(0) \; Q(0)]^T$. To complete the analysis of the proposed attitude control system, it is necessary to verify that applying feedback in Eq. (8) to system in Eqs. (1)-(4), it does not occur that variables U and W diverge to infinity in finite time. Let $[\Theta(t) \; Q(t)]^T$ be the generic solution of Eqs. (7) and (8), and let $\Delta(t)$ be the corresponding time behavior of control input Δ. Because of the previous theorem, all those functions are defined for all $t \geq 0$ and are continuos. Then, from Eqs. (1) and (2) obtain that $[U \; W]^T$ is solution to the following linear time-varying nonhomogeneous system of differential equations

$$\begin{bmatrix} \dot{U} \\ \dot{W} \end{bmatrix} = \begin{bmatrix} 0 & -Q(t) \\ Q(t) & 0 \end{bmatrix} \begin{bmatrix} U \\ W \end{bmatrix} + \begin{bmatrix} -g\cos(\Theta(t)) + \dfrac{T_c \cos(\text{sat}_{\overline{\Delta}}(\Delta(t)))}{m} \\ -g\sin(\Theta(t)) + \dfrac{T_c \sin(\text{sat}_{\overline{\Delta}}(\Delta(t)))}{m} \end{bmatrix} \tag{12}$$

It is well know that for any initial value $[U(0) \; W(0)]^T$ the solution $[U(t) \; W(t)]^T$ of system (12) is continuous and defined for all $t \geq 0$ (see [16, Chapter 1]).

The study performed so far leads to the following main proposition.

Proposition 1. *Consider the launch vehicle described by Eqs. (1)-(4). Apply the PD autopilot in Eq. (8). Then, if Θ_c is constant, for any initial condition $[U(0) \; W(0) \; Q(0) \; \Theta(0)]^T$, it occurs that $\Theta(t) \to \Theta_c$ for $t \to \infty$.*

Note that the above result holds regardless of the values of constant parameters I, l_c, m and T_c. Consequently, the PD autopilot is robust with respect to uncertainties of those parameters. Moreover, it is only required that feedback gains satisfy $k_p > 0$ and $k_d > 0$. In practice, k_p and k_d are selected so to obtain satisfactory transient performance. For that purpose it is important to

know the range of variability of parameter $G = l_c T_c / I$. The latter point will be illustrated in the case study presented in section 5.

Note that a standard design based on linearization of Eq. (7) about $[\Theta\ Q]^T = [\Theta_c\ 0]^T$ and $\Delta = 0$, leads to the same control law as in Eq. (8) (see [1, Section 5.3.1.1]). Consequently, it was already known that local convergence is achieved by using PD control. However, the contribution of this study is showing that PD control actually achieves global convergence and does it robustly with respect to uncertainties in the parameters.

4. Autopilot Design Including the Dynamics of the Actuator

In case the actuator is not much faster than the autopilot, it is important to take its effects into account in the autopilot design process. In fact, if that is not the case, the influence of the actuator can lower substantially the performance of the autopilot. As a result, in this section the autopilot design is carried out including the servoactuator model in Eq. (6).

Consider only Eqs. (3), (4), and (6) since they are decoupled from equations (1) and (2). Then, using again $\widetilde{\Theta} = \Theta - \Theta_c$ with Θ_c constant, the former equations can be rewritten as follows

$$\dot{\widetilde{\Theta}} = Q \tag{13}$$

$$\dot{Q} = G \sin(\mathrm{sat}_{\overline{\Delta}}(\Delta)) \tag{14}$$

$$\dot{\Delta} = -\frac{1}{\tau_a}\Delta + \frac{1}{\tau_a}\Delta_c \tag{15}$$

The objective is designing a feedback law for Δ_c that makes $\widetilde{\Theta} \to 0$ for any initial condition $[\widetilde{\Theta}(0)\ Q(0)\ \Delta(0)]^T$. Measures of $\widetilde{\Theta}$, Q, and Δ are considered available to the autopilot. Moreover, the design must be robust with respect to the following parametric uncertainties $\underline{G} \leq G \leq \overline{G}$, $\underline{\tau}_a \leq \tau_a \leq \overline{\tau}_a$.

The design can be executed by following a backstepping approach. The backstepping design is a recursive procedure which allows to solve a stabilization problem in several steps considering at each step a subsystem of increasing dimension. Backstepping design for systems subject to parametric uncertainties,

known as robust backstepping, is outlined in section 11.1 of [17]. The latter approach is summarized in a simplified fashion in the forthcoming subsection 4.2. However, first it is helpful to present some results on input-to-state stability of uncertain nonlinear systems.

4.1. Results on Input-to-state Stability of Uncertain Nonlinear Systems

For the rest of the paper it is useful to recall that a continuous scalar function $\alpha(r)$ defined for $0 \leq r < a$, is class $\mathcal{K}$ if $\alpha(0) = 0$ and $\alpha(r)$ is strictly increasing. If in addition $a = \infty$ and $\lim_{r\to\infty} \alpha(r) = \infty$, then α is class $\mathcal{K}_\infty$. A continuos scalar function $\beta(r, t)$ defined for $0 \leq r < a$ and $t \geq 0$ is class $\mathcal{KL}$, if $\beta(\cdot, t) \in \mathcal{K}$ for all $t \geq 0$ and $\lim_{t\to\infty} \beta(r, t) = 0$ for all $0 \leq r < a$.

Consider system

$$\dot{x} = f(x, u, \mu) \tag{16}$$

in which $x \in \mathbb{R}^n$ is the state, $u \in \mathbb{R}^m$ is the control input, and $\mu \in \mathbb{R}^p$ is a vector of unknown constant parameters. It is only known that $\mu \in \mathcal{P}$ where $\mathcal{P}$ is a subset of $\mathbb{R}^p$. Assume that f is a locally Lipschitz function such that $f(0, 0, \mu) = 0$ for all $\mu \in \mathcal{P}$. Then, when $u = 0$, $x = 0$ is an equilibrium for all possible values of μ. Consider any piecewise continuous input function $u(t)$ with $t \geq 0$ and define $\|u(\cdot)\| = \sup_{t\geq 0} \|u(t)\|$. System in Eq. (16) is *robustly input-to-state-stable* (see [18]) if there exists $\beta \in \mathcal{KL}$ and $\gamma \in \mathcal{K}$, such that for any piecewise continuos input $u(t)$, for any initial state $x(0) = x_0 \in \mathbb{R}^n$, and for any value of the unknown parameter $\mu \in \mathcal{P}$, the corresponding state response $x(t)$ fulfills the following

$$\|x(t)\| \leq \beta(\|x_0\|, t) + \gamma(\|u(\cdot)\|) \qquad \forall t \geq 0$$

Function γ is called *iss-gain* of system in Eq. (16).

A useful sufficient condition for robust input-to-state stability is given by in the following Lyapunov-type theorem (see proposition 3.3 of [18] and theorem 10.4.1 of [17]).

Theorem 2. *Suppose there exists a continuously differentiable scalar function $V(x, \mu)$ with $x \in \mathbb{R}^n$ and $\mu \in \mathcal{P}$ for which it is possible to find three class $\mathcal{K}_\infty$*

functions $\underline{\alpha}$, $\overline{\alpha}$, α *and a class* $\mathcal{K}$ *function* χ *such that the following relations hold true*

$$\underline{\alpha}(\|x\|) \leq V(x,\mu) \leq \overline{\alpha}(\|x\|) \qquad \forall x \in \mathbb{R}^n \qquad \forall \mu \in \mathcal{P}$$

$$\|x\| \geq \chi(\|u\|) \;\Rightarrow\; \frac{\partial V}{\partial x}(x,\mu) f(x,u,\mu) \leq -\alpha(\|x\|) \qquad \forall \mu \in \mathcal{P}$$

Then, system in Eq. (16) is robustly input-to-state stable with iss-gain

$$\gamma(r) = \underline{\alpha}^{-1} \circ \overline{\alpha} \circ \chi(r) \tag{17}$$

4.2. Results on Global Stabilization of Uncertain Nonlinear Systems via Robust Backstepping

The focus of the current subsection is presenting the robust backstepping approach for stabilization of uncertain nonlinear systems of the following type

$$\dot{z} = f_z(z,\Delta,\mu) \tag{18}$$

$$\dot{\Delta} = q(z,\Delta,\mu) + b(z,\Delta,\mu)\Delta_c \tag{19}$$

In the above equations $z \in \mathbb{R}^n$ and $\Delta \in \mathbb{R}$ are state variables, $\Delta_c \in \mathbb{R}$ is the control input, and $\mu \in \mathbb{R}^p$ is a vector of unknown constant parameters. It is only known that $\mu \in \mathcal{P}$ where $\mathcal{P}$ is a subset of $\mathbb{R}^p$. Assume that f_z, q, and b are locally Lipschitz functions, and that $f_z(0,0,\mu) = 0$ and $q(0,0,\mu) = 0$ for all $\mu \in \mathcal{P}$. Then, when $\Delta_c = 0$, $[z\ \Delta]^T = [0\ 0]^T$ is an equilibrium for all possible values of μ. Moreover, assume that for some $b_0 > 0$ it holds that $b(z,\Delta,\mu) \geq b_0$ for all $z \in \mathbb{R}^n$, $\Delta \in \mathbb{R}$, $\mu \in \mathcal{P}$. The objective is designing a feedback that, using measures of z and Δ (state feedback), makes $[z\ \Delta]^T = [0\ 0]^T$ become a globally asymptotically stable equilibrium for all $\mu \in \mathcal{P}$.

The feedback design is performed in two phases. In the first phase consider only Eq. (18), and imagine that Δ is a (virtual) control input. Then, the goal of the first phase is designing a (virtual) feedback $\Delta = v^*(z) + \beta^*(z)y$. In the previous equation $v^*(z)$ and $\beta^*(z)$ are scalar continuously differentiable functions fulfilling $0 < \beta^*(z) \leq \beta_0^*$ for all $z \in \mathbb{R}^n$, and y is a scalar variable. The feedback must be designed so that the resulting (virtual) closed-loop system $\dot{z} = f_z(z, v^*(z) + \beta^*(z)y, \mu)$ is robustly input-to-state-stable with respect to

input y, state z, and uncertain parameter μ. It is also required that the iss-gain γ_z of the obtained closed-loop system is a continuously differentiable class $\mathcal{K}_\infty$ function. Next, it is necessary to determine a continuously differentiable $\overline{\gamma}_z \in \mathcal{K}_\infty$ such that

$$\gamma_z(r) < \overline{\gamma}_z(r) \quad \forall r > 0 \tag{20}$$

Once the first phase is completed, in Eqs. (18) and (19) the state variable Δ is replaced by the new variable $y = (\beta^*(z))^{-1}(\Delta - v^*(z))$ so to obtain

$$\dot{z} = \tilde{f}_z(z, y, \mu) \tag{21}$$

$$\dot{y} = \tilde{q}(z, y, \mu) + \tilde{b}(z, y, \mu)\Delta_c \tag{22}$$

where

$$\tilde{f}_z(z, y, \mu) = f_z(z, v^*(z) + \beta^*(z)y, \mu)$$

$$\tilde{q}(z, y, \mu) = \frac{1}{\beta^*(z)} \left(q(z, v^*(z) + \beta^*(z)y, \mu) - \frac{\partial v^*}{\partial z}(z)\tilde{f}_z(z, y, \mu) - \frac{\partial \beta^*}{\partial z}(z)\tilde{f}_z(z, y, \mu)y \right)$$

$$\tilde{b}(z, y, \mu) = \frac{1}{\beta^*(z)} b(z, v^*(z) + \beta^*(z)y, \mu) \tag{23}$$

160 Next, it is presented how to design a feedback that globally stabilizes system in Eqs. (21) and (22) for all $\mu \in \mathcal{P}$.

Assume that it is possible to find $\eta_0 \in \mathcal{K}$ and $\eta_1 \in \mathcal{K}$, with η_0 and η_1 continuously differentiable, such that

$$|\tilde{q}(z, y, \mu)| \leq \eta_0(|y|) + \eta_1(\|z\|) \quad \forall z \in \mathbb{R}^n \quad \forall y \in \mathbb{R} \quad \forall \mu \in \mathcal{P} \tag{24}$$

Then, find a continuously differentiable function $\kappa(y)$ that satisfies the following three conditions

1. $\kappa(y)$ restricted to $y \geq 0$ is a class $\mathcal{K}_\infty$ function
2. $\kappa(y) \geq \frac{2}{\tilde{b}_0}(\eta_0(y) + \eta_1(\overline{\gamma}_z(y))) \quad \forall y \geq 0$ (25)

$$3.\ \ \kappa(-y) = -\kappa(y) \quad \forall y \in \mathbb{R} \tag{26}$$

Thus, the following theorem, obtained by adapting lemma 11.4.1 of [17] (see also [19]), holds true.

Theorem 3. *For system in Eqs. (21) and (22), feedback* $\Delta_c = -\kappa(y)$ *makes equilibrium* $[z\ y]^T = [0\ 0]^T$ *globally asymptotically stable for all* $\mu \in \mathcal{P}$.

Then, based on the previous results, it follows that the following memory-less state feedback

$$\Delta_c = -\kappa((\beta^*(z))^{-1}(\Delta - v^*(z)))$$

applied to system in Eqs. (18) and (19), makes its origin a globally asymptotically stable equilibrium for all $\mu \in \mathcal{P}$.

4.3. Autopilot Design

The current subsection presents the design of a feedback that globally asymptotically stabilizes the origin of system in Eqs. (13) - (15) subject to the following parametric uncertainties $\underline{G} \leq G \leq \overline{G}$, $\underline{\tau}_a \leq \tau_a \leq \overline{\tau}_a$. The design is based on the robust backstepping method outlined in the previous subsection.

Let $z \triangleq [\widetilde{\Theta}\ Q]^T$, and represent Eqs. (13) and (14) in the following concise form

$$\dot{z} = f_z(z, \Delta, G) \tag{27}$$

where

$$f_z(z, \Delta, G) = \begin{bmatrix} Q \\ G\sin(\mathrm{sat}_{\overline{\Delta}}(\Delta)) \end{bmatrix} \tag{28}$$

The goal of the first phase is determining a (virtual) feedback $\Delta = v^*(z) + \beta^*(z)y$. In the previous equation $v^*(z)$ and $\beta^*(z)$ are scalar continuously differentiable functions fulfilling $0 < \beta^*(z) \leq \beta_0^*$ for all $z \in \mathbb{R}^2$, and y is a scalar variable. The feedback must be designed so that the resulting (virtual) closed-loop system

$$\dot{z} = f_z(z, v^*(z) + \beta^*(z)y, G) \tag{29}$$

is robustly input-to-state-stable with input y, state z, and uncertain parameter $\underline{G} \leq G \leq \overline{G}$. By theorem 2, this is achieved if we can find $v^*(z)$, $\beta^*(z)$, and $V_z(z, G)$ such that there exist three class $\mathcal{K}_\infty$ functions $\underline{\alpha}_z$, $\overline{\alpha}_z$, α_z, and a class $\mathcal{K}$ function χ_z so that the following equations hold true

$$\underline{\alpha}_z(\|z\|) \leq V_z(z, G) \leq \overline{\alpha}_z(\|z\|) \quad \forall z \in \mathbb{R}^2 \;\; \forall G \in [\underline{G}\ \overline{G}] \tag{30}$$

$$\|z\| \geq \chi_z(|y|) \;\Rightarrow\; \frac{\partial V_z}{\partial z}(z, G) f_z(z, v^*(z) + \beta^*(z) y, G) \leq -\alpha_z(\|z\|) \quad \forall G \in [\underline{G}\ \overline{G}] \tag{31}$$

Setting $y = 0$ in Eq. (31), obtain

$$\frac{\partial V_z}{\partial z}(z, G) f_z(z, v^*(z), G) \leq -\alpha_z(\|z\|) \;\; \forall G \in [\underline{G}\ \overline{G}] \tag{32}$$

Thus, as first step search for $v^*(z)$ and $V_z(z, G)$ such that there exist class $\mathcal{K}_\infty$ functions $\underline{\alpha}_z$, $\overline{\alpha}_z$, α^* that fulfill Eq. (30) as well as the following inequality

$$\frac{\partial V_z}{\partial z}(z, G) f_z(z, v^*(z), G) \leq -\alpha^*(\|z\|) \;\; \forall G \in [\underline{G}\ \overline{G}] \tag{33}$$

The function α^* is introduced at this stage since it will be different from the function α_z that will fulfill Eq. (31).

Clearly Eqs. (30) and (33) imply that equilibrium $z = 0$ is globally asymptotically stable for system $\dot{z} = f_z(z, v^*(z), G)$ for all $\underline{G} \leq G \leq \overline{G}$. Then, because of theorem 1 it seems natural picking $v^*(z) = -(k_p \widetilde{\Theta} + k_d Q)$ and $V_z(z, G)$ as in Eq. (10). However, Eq. (11) shows that with the latter choice, the left-hand side of Eq. (33) is not negative definite with respect to z. Consequently, a class $\mathcal{K}_\infty$ function α^* that makes (33) hold true cannot exist. As a result, the proposed choice for v^* and V_z is not valid. Then, inspired by example 3.2 in [20], set

$$v^*(z) = -\arcsin(\sigma(k_p \widetilde{\Theta} + k_d Q)) \tag{34}$$

where

$$\sigma(r) \triangleq \frac{2 \sin \overline{\Delta}}{\pi} \arctan\left(\frac{\pi}{2 \sin \overline{\Delta}} r\right) \tag{35}$$

Function σ represents a smooth, strictly increasing modification of the saturation function defined in (5) with saturation limit equal to $\sin\overline{\Delta}$ instead of $\overline{\Delta}$. Introduce $\Phi(r) \triangleq \int_0^r \sigma(s)ds$, and define

$$V^\circ(z,G) \triangleq G(\Phi(k_p\widetilde{\Theta}) + \Phi(k_p\widetilde{\Theta} + k_dQ)) + k_pQ^2 \tag{36}$$

In Appendix A it is shown that

$$\underline{\alpha}^\circ(\|z\|) \leq V^\circ(z,G) \leq \overline{\alpha}^\circ(\|z\|) \quad \forall z \in \mathbb{R}^2 \;\; \forall G \in [\underline{G}\;\overline{G}] \tag{37}$$

where $\underline{\alpha}^\circ$ and $\overline{\alpha}^\circ$ are the following class $\mathcal{K}_\infty$ functions

$$\underline{\alpha}^\circ(r) = \frac{\underline{\alpha}_0^\circ r^2}{1+\underline{\alpha}_1^\circ r} \qquad \overline{\alpha}^\circ(r) = \overline{\alpha}_0^\circ r^2 \tag{38}$$

with coefficients $\underline{\alpha}_0^\circ > 0$, $\underline{\alpha}_1^\circ > 0$, and $\overline{\alpha}_0^\circ > 0$ defined in Appendix A.

Next, note that the expression of $f_z(z, v^*(z), G)$ can be simplified as follows

$$f_z(z, v^*(z), G) = \begin{bmatrix} Q \\ -G\sigma(k_p\widetilde{\Theta} + k_dQ) \end{bmatrix}$$

and consequently

$$\frac{\partial V^\circ}{\partial z}(z,G) f_z(z, v^*(z), G) = -Gk_pQ(\sigma(k_p\widetilde{\Theta} + k_dQ) - \sigma(k_p\widetilde{\Theta})) \\ - G^2k_d\sigma^2(k_p\widetilde{\Theta} + k_dQ) \tag{39}$$

In Appendix B it is shown that

$$\frac{\partial V^\circ}{\partial z}(z,G) f_z(z, v^*(z), G) \leq -\alpha^\circ(\|z\|) \quad \forall z \in \mathbb{R}^2 \;\; \forall G \in [\underline{G}\;\overline{G}] \tag{40}$$

where

$$\alpha^\circ(r) = \frac{\alpha_0^\circ r^2}{1+\alpha_1^\circ r^2}$$

with $\alpha_0^\circ > 0$ and $\alpha_1^\circ > 0$ defined in Appendix B. Note that function $\alpha^\circ \in \mathcal{K}$, and it is not possible to find $\alpha^\circ \in \mathcal{K}_\infty$ that makes Eq. (40) fulfilled. In fact, Eq. (39) shows that the left hand side of Eq. (40) is not radially unbounded with respect to z. Consequently, setting $v^*(z)$ as in Eq. (34) and $V_z(z,G) = V^\circ(z,G)$ as in Eq. (36) is not a valid choice for fulfilling Eq. (33) since it is required that

$\alpha^* \in \mathcal{K}_\infty$. However, based on remark 10.1.4 of [17], keeping $v^*(z)$ as in Eq. (34) and setting

$$V_z(z,G) = \frac{1}{2}(V^\circ(z,G))^2 \tag{41}$$

it is possible to fulfill both Eqs. (30) and (33). In fact, clearly Eq. (30) is satisfied by picking

$$\underline{\alpha}_z(r) = \frac{1}{2}(\underline{\alpha}^\circ(r))^2 = \left(\frac{\underline{\alpha}_{z0} r^2}{1+\underline{\alpha}_{z1} r}\right)^2 \qquad \overline{\alpha}_z(r) = \frac{1}{2}(\overline{\alpha}^\circ(r))^2 = \overline{\alpha}_{z0} r^4$$

where $\underline{\alpha}_{z0} = \underline{\alpha}_0^\circ/\sqrt{2}$, $\underline{\alpha}_{z1} = \underline{\alpha}_1^\circ$, and $\overline{\alpha}_{z0} = (\overline{\alpha}_0^\circ)^2/2$. Moreover, the following holds true

$$\begin{aligned}\frac{\partial V_z}{\partial z}(z,G) f_z(z, v^*(z), G) &= V^\circ(z,G)\frac{\partial V^\circ}{\partial z}(z,G) f_z(z, v^*(z), G) \\ &\leq -\underline{\alpha}^\circ(\|z\|)\alpha^\circ(\|z\|) \quad \forall z \in \mathbb{R}^2 \;\; \forall G \in [\underline{G}\ \overline{G}]\end{aligned}$$

As a result, Eq. (33) is satisfied by setting

$$\alpha^*(r) = \underline{\alpha}^\circ(r)\alpha^\circ(r) = \frac{\alpha_0^* r^4}{1+\alpha_1^* r + \alpha_2^* r^2 + \alpha_3^* r^3}$$

with $\alpha_0^* = \underline{\alpha}_0^\circ \alpha_0^\circ$, $\alpha_1^* = \underline{\alpha}_1^\circ$, $\alpha_2^* = \alpha_1^\circ$, and $\alpha_3^* = \underline{\alpha}_1^\circ \alpha_1^\circ$. It is important to note
180 that the above function is class $\mathcal{K}_\infty$ since $\underline{\alpha}^\circ \in \mathcal{K}_\infty$ and $\alpha^\circ \in \mathcal{K}$.

Next objective is finding a continuously differentiable $\beta^*(z)$ such that $0 < \beta^*(z) \leq \beta_0^*$ for all $z \in \mathbb{R}^2$ and for which it is possible to determine $\alpha_z \in \mathcal{K}_\infty$ and $\chi_z \in \mathcal{K}$ so that Eq. (31) holds.

For that purpose note that

$$\begin{aligned}\frac{\partial V_z}{\partial z}(z,G) f_z(z, v^*(z)+\beta^*(z)y, G) &= \frac{\partial V_z}{\partial z}(z,G) f_z(z, v^*(z), G) + \\ &\frac{\partial V_z}{\partial z}(z,G)(f_z(z, v^*(z)+\beta^*(z)y, G) - f_z(z, v^*(z), G)) \leq \\ &-\alpha^*(\|z\|) + \frac{\partial V_z}{\partial z}(z,G)\begin{bmatrix} 0 \\ Gp(z,\beta^*(z)y)\end{bmatrix}\end{aligned}$$

where

$$p(z,y') = \sin(\mathrm{sat}_{\overline{\Delta}}(v^*(z)+y')) - \sin(\mathrm{sat}_{\overline{\Delta}}(v^*(z)))$$

Thus

$$\frac{\partial V_z}{\partial z}(z,G)f_z(z,v^*(z)+\beta^*(z)y,G) \leq -\alpha^*(\|z\|)+\left|\frac{\partial V_z}{\partial Q}(z,G)\right|\overline{G}|p(z,\beta^*(z)y)|$$

It is easy to obtain that $|p(z,y')| \leq |y'|$, and in Appendix C it is shown that

$$\left|\frac{\partial V_z}{\partial Q}(z,G)\right| \leq \widehat{\alpha}(\|z\|) \quad \forall z \in \mathbb{R}^2 \;\; \forall G \in [\underline{G}\;\overline{G}] \tag{42}$$

with $\widehat{\alpha}(r)=\widehat{\alpha}_0 r^3$ where $\widehat{\alpha}_0 > 0$ is defined in Appendix C. Consequently

$$\begin{aligned}\frac{\partial V_z}{\partial z}(z,G)f_z(z,v^*(z)+\beta^*(z)y,G) \leq -\frac{1}{2}\alpha^*(\|z\|)-\frac{1}{2}\alpha^*(\|z\|)\\ +\overline{G}\widehat{\alpha}(\|z\|)|\beta^*(z)||y| \quad \forall z \in \mathbb{R}^2 \;\; \forall G \in [\underline{G}\;\overline{G}]\end{aligned}$$

Thus, clearly Eq. (31) is fulfilled with $\alpha_z(r)=\alpha^*(r)/2$, if we can find $\chi_z \in \mathcal{K}$ and a continuously differentiable $\beta^*(z)$ with $0<\beta^*(z)\leq\beta_0^*$ for all $z \in \mathbb{R}^2$, such that

$$\|z\| \geq \chi_z(|y|) \;\Rightarrow\; -\frac{1}{2}\alpha^*(\|z\|)+\overline{G}\widehat{\alpha}(\|z\|)|\beta^*(z)||y| \leq 0$$

Then, it is convenient to restrict the search to $\chi_z \in \mathcal{K}_\infty$ rather than $\chi_z \in \mathcal{K}$. In fact, in that case the equation above is equivalent to

$$\chi_z^{-1}(\|z\|) \geq |y| \;\Rightarrow\; \frac{1}{2}\alpha^*(\|z\|) \geq \overline{G}\widehat{\alpha}(\|z\|)|\beta^*(z)||y|$$

Clearly, the above equation holds true if β^* and $\chi_z^{-1} \in \mathcal{K}_\infty$ are selected so that the following is satisfied

$$\frac{1}{2}\alpha^*(\|z\|) \geq \overline{G}\widehat{\alpha}(\|z\|)|\beta^*(z)|\chi_z^{-1}(\|z\|) \quad \forall z \in \mathbb{R}^2 \tag{43}$$

Thus, proceed as follows. Set $\beta^*(z)=1/(1+\|z\|^2)^\nu$ where ν is a positive integer to be determined later. Note that the proposed β^* is continuously differentiable and is such that $0<\beta^*(z)\leq\beta_0^*=1$, as required. For small $\|z\|$ Eq. (43) can be approximated as follows

$$\frac{1}{2}\alpha_0^*\|z\|^4 \geq \overline{G}\widehat{\alpha}_0\|z\|^3\chi_z^{-1}(\|z\|)$$

Clearly, the previous inequality can be satisfied by picking

$$\chi_z^{-1}(r)=\frac{1}{\chi_{z0}}r \tag{44}$$

with $\chi_{z0} > 0$ and sufficiently large. Consequently, set χ_z^{-1} as in Eq. (44), and note that for large $\|z\|$, Eq. (43) can be approximated as follows

$$\frac{1}{2}\frac{\alpha_0^*}{\alpha_3^*}\|z\| \geq \overline{G}\widehat{\alpha}_0\|z\|^3\|z\|^{-2\nu}\frac{1}{\chi_{z0}}\|z\|$$

Clearly setting $\nu = 2$ makes the above inequality fulfilled for $\|z\|$ sufficiently large. Thus, set $\beta^*(z) = 1/(1+\|z\|^2)^2$ and χ_z^{-1} as in Eq. (44), and see if it possible to find $\chi_{z0} > 0$ so that Eq. (43) holds true. The latter equation is equivalent to

$$\frac{\alpha_0^* r^4}{2(1+\alpha_1^* r + \alpha_2^* r^2 + \alpha_3^* r^3)} \geq \frac{\overline{G}\widehat{\alpha}_0 r^4}{\chi_{z0}(1+r^2)^2} \quad \forall r \geq 0$$

The previous inequality holds true if and only if $q_1(r)r^2 + q_2(r) \geq 0$ for all $r \geq 0$ where q_1 and q_2 are the following quadratic polynomials

$$\begin{aligned} q_1(r) &= \alpha_0^*\chi_{z0}r^2 - 2\overline{G}\widehat{\alpha}_0\alpha_3^* r + \alpha_0^*\chi_{z0} - \overline{G}\widehat{\alpha}_0\alpha_2^* \\ q_2(r) &= (\alpha_0^*\chi_{z0} - \overline{G}\widehat{\alpha}_0\alpha_2^*)r^2 - 2\overline{G}\widehat{\alpha}_0\alpha_1^* r + \alpha_0^*\chi_{z0} - 2\overline{G}\widehat{\alpha}_0 \end{aligned}$$

It is easy to verify that the following condition

$$\chi_{z0} = \frac{\overline{G}\widehat{\alpha}_0}{2\alpha_0^*}\max\left\{\alpha_2^* + \sqrt{(\alpha_2^*)^2 + 4\alpha_3^*}\ ,\ \alpha_2^* + 2 + \sqrt{(\alpha_2^* - 2)^2 + 4\alpha_1^*}\right\}$$

guarantees that $q_1(r) \geq 0$ and $q_2(r) \geq 0$ for all r. In conclusion, setting $\beta^*(z) = 1/(1+\|z\|^2)^2$, $\alpha_z(r) = \alpha^*(r)/2$, and $\chi_z(r) = \chi_{z0}r$ with χ_{z0} as in the above equation, makes Eq. (31) fulfilled. As a result, by Eq. (17) the iss-gain of system in Eq. (29) is given by

$$\gamma_z(r) = \underline{\alpha}_z^{-1} \circ \overline{\alpha}_z \circ \chi_z(r) = \frac{\chi_{z0} r}{2\underline{\alpha}_{z0}}\left(\sqrt{4\underline{\alpha}_{z0}\sqrt{\overline{\alpha}_{z0}} + \underline{\alpha}_{z1}^2\overline{\alpha}_{z0}\chi_{z0}^2 r^2} + \underline{\alpha}_{z1}\sqrt{\overline{\alpha}_{z0}}\chi_{z0} r\right)$$

Note that γ_z is class $\mathcal{K}_\infty$ and continuously differentiable as required. Next, determine continuously differentiable $\overline{\gamma}_z \in \mathcal{K}_\infty$ such that

$$\gamma_z(r) < \overline{\gamma}_z(r) \quad \forall r > 0 \tag{45}$$

For that purpose note that

$$\sqrt{4\underline{\alpha}_{z0}\sqrt{\overline{\alpha}_{z0}} + \underline{\alpha}_{z1}^2\overline{\alpha}_{z0}\chi_{z0}^2 r^2} < 2\sqrt{\underline{\alpha}_{z0}}(\overline{\alpha}_{z0})^{1/4} + \underline{\alpha}_{z1}\sqrt{\overline{\alpha}_{z0}}\chi_{z0} r \quad \forall r > 0$$

Thus, it can be set

$$\overline{\gamma}_z(r) = \overline{\gamma}_{z1} r + \overline{\gamma}_{z2} r^2 \tag{46}$$

with $\overline{\gamma}_{z1} = (\overline{\alpha}_{z0})^{1/4}\chi_{z0}/\sqrt{\underline{\alpha}_{z0}}$ and $\overline{\gamma}_{z2} = \underline{\alpha}_{z1}\sqrt{\overline{\alpha}_{z0}}\chi_{z0}^2/\underline{\alpha}_{z0}$.

Consider now Eqs. (15) and (27) and change variable Δ into

$$y = (\beta^*(z))^{-1}(\Delta - v^*(z)) \tag{47}$$

obtaining

$$\begin{aligned} \dot{z} &= \tilde{f}_z(z, y, G) \\ \dot{y} &= \tilde{q}(z, y, G, \tau_a) + \tilde{b}(z, \tau_a)\Delta_c \end{aligned} \tag{48}$$

where

$$\tilde{f}_z(z, y, G) = f_z(z, v^*(z) + \beta^*(z)y, G)$$

$$\tilde{q}(z, y, G, \tau_a) = -\frac{1}{\beta^*(z)}\left(\frac{1}{\tau_a}v^*(z) + \frac{\partial v^*}{\partial z}(z)\tilde{f}_z(z, y, G) + \frac{\partial \beta^*}{\partial z}(z)\tilde{f}_z(z, y, G)y\right) - \frac{1}{\tau_a}y \tag{49}$$

$$\tilde{b}(z, \tau_a) = \frac{1}{\tau_a \beta^*(z)} \tag{50}$$

Clearly

$$\tilde{b}(z, \tau_a) \geq \tilde{b}_0 = \frac{1}{\overline{\tau}_a} \quad \forall z \in \mathbb{R}^2 \quad \forall \tau_a \in [\underline{\tau}_a\ \overline{\tau}_a] \tag{51}$$

Moreover, it is shown in Appendix D that

$$|\tilde{q}(z, y, G, \tau_a)| \leq \eta_0(|y|) + \eta_1(\|z\|) \qquad \forall z \in \mathbb{R}^2 \ \ \forall y \in \mathbb{R} \quad \forall G \in [\underline{G}\ \overline{G}] \quad \forall \tau_a \in [\underline{\tau}_a\ \overline{\tau}_a] \tag{52}$$

with

$$\eta_0(r) = \eta_{01} r + \eta_{02} r^2 + \eta_{04} r^4 \quad \eta_1(r) = \eta_{11} r + \eta_{12} r^2 + \eta_{13} r^3 + \eta_{14} r^4 + \eta_{15} r^5 \tag{53}$$

where coefficients $\eta_{0i} > 0$ $i = 1, 2, 4$ and $\eta_{1i} > 0$ $i = 1, \ldots, 5$ are defined in Appendix D.

Then, denote the function that appears on the right-hand side of Eq. (25) as

$$\underline{\kappa}(r) \triangleq \frac{2}{\widetilde{b}_0}(\eta_0(r) + \eta_1(\overline{\gamma}_z(r))) \qquad r \geq 0$$

From Eqs. (46) and (53) it is straightforward to obtain that $\underline{\kappa}(r) = \sum_{i=1}^{10} \underline{\kappa}_i r^i$ where the expressions of $\underline{\kappa}_i > 0 \;\; i = 1, \ldots, 10$ can be easily determined. Then, a function $\kappa(y)$ that fulfills all required properties indicated in subsection 4.2 is given by

$$\kappa(y) = \sum_{i=1}^{10} \underline{\kappa}_i |y|^i \mathrm{sgn}(y) \tag{54}$$

Thus, by theorem 3 it follows that for system in Eqs. (13)-(15) feedback $\Delta_c = -\kappa(y)$ makes $[\widetilde{\Theta} \;\; Q \;\; \Delta]^T = [0 \;\; 0 \;\; 0]^T$ a robustly globally asymptotically stable equilibrium. Moreover, repeating the same argument as in section 3, it is guaranteed that variables U and W that fulfill Eqs. (1) and (2) do not diverge to infinity in finite time. Thus, the following concluding proposition can be stated.

Proposition 2. *Consider the launch vehicle described by Eqs. (1)-(4) and (6). Apply the nonlinear memory-less state feedback $\Delta_c = -\kappa(y)$ in which $\kappa(y)$ is given by Eq. (54) and*

$$y = (1 + (\Theta - \Theta_c)^2 + Q^2)^2 \left(\Delta + \arcsin(\sigma(k_p(\Theta - \Theta_c) + k_d Q))\right) \tag{55}$$

where σ is defined in Eq. (35). Then, if Θ_c is constant, for any initial condition $[U(0) \;\; W(0) \;\; Q(0) \;\; \Theta(0) \;\; \Delta(0)]^T$ and for any $m > 0$, $\underline{I} \leq I \leq \overline{I}$, $\underline{l_c} \leq l_c \leq \overline{l_c}$, $\underline{T_c} \leq T_c \leq \overline{T_c}$ and $\underline{\tau_a} \leq \tau_a \leq \overline{\tau_a}$, it occurs that $\Theta(t) \to \Theta_c$ for $t \to \infty$.

Thus, the proposed autopilot guarantees global convergence to the desired attitude robustly with respect to parametric uncertainties.

5. Case Study

Consider the following data for a launch vehicle flying above atmospheric level. Distance l_c, inertia moment I, and mass m vary with time as follows

$$l_c = l_{ci} + \dot{l}_c t \quad I = I_i + \dot{I} t \quad m = m_i + \dot{m} t \tag{56}$$

where $l_{ci} = 1$ m, $\dot{l}_c = 8.70 \cdot 10^{-4}$ m/s, $I_i = 9200$ kg m^2, $\dot{I} = -7.83$ kg m^2/s, $m_i = 4700$ kg, $\dot{m} = -3.84$ kg/s. The flight time is set equal to $t_f = 575$ sec. Thus, at final time t_f the previous parameters become equal to $l_{cf} = 1.5$ m, $I_f = 4700$ kg m^2, $m_f = 2492$. For autopilot design purposes, parameters l_c, I, and m are considered constant since their speed of variation will be much slower compared to the speed of convergence that the autopilots will achieve. However, since they vary with time, their values are uncertain and range on the following intervals $l_{ci} = \underline{l_c} \leq l_c \leq \overline{l_c} = l_{cf}$, $I_f = \underline{I} \leq I \leq \overline{I} = I_i$, $m_f = \underline{m} \leq m \leq \overline{m} = m_i$. The thrust is constant with nominal value $T_{c0} = 1.15 \cdot 10^4$ N, and is subject to 10 % uncertainty. Thus, $1.04 \cdot 10^4$ N $= \underline{T_c} \leq T_c \leq \overline{T_c} = 1.27 \cdot 10^4$ N. The maximum amplitude of the engine deflection angle is equal to $\overline{\Delta} = 10$ deg.

5.1. Autopilot Design not Including the Dynamics of the Actuator.

Here the servoactuator model is not considered for autopilot design. Consequently, the proposed design is effective if the actuator is much faster than the resulting attitude controller. In section 3 it has been shown that a global robust autopilot is given by Eq. (8). In order to determine appropriate values for the positive gains k_p and k_d, proceed as follows. Consider the linear approximation of closed-loop system in Eqs. (7) and (8) about equilibrium $[\Theta \ Q]^T = [\Theta_c \ 0]^T$. The latter approximation is given by

$$\begin{aligned} \dot{\Theta} &= Q \\ \dot{Q} &= G(k_p(\Theta_c - \Theta) - k_d Q) \end{aligned} \tag{57}$$

Thus, in the Laplace domain

$$\frac{\widehat{\Theta}(s)}{\widehat{\Theta}_c(s)} = \frac{Gk_p}{s^2 + Gk_d s + Gk_p} \tag{58}$$

Determine k_p and k_d so that the step response of (58) fulfills the following specifications: maximum percentage overshoot $M_p \leq 2\%$, settling time $t_s \leq 10$ sec, and rise time $t_r \leq 5$ sec. The specifications must be fulfilled for all values of parameter G within its variability range $\underline{G} \leq G \leq \overline{G}$.

Using standard results (see [21, Chapter 7]), it can be obtained that the specifications are likely to be satisfied if transfer function (58) possesses poles

having damping ratio $\zeta \geq \underline{\zeta} = 0.8$ and natural angular frequency $\omega_n \geq \underline{\omega_n} = 0.7$ rad/s for all $\underline{G} \leq G \leq \overline{G}$. Since $k_p G = \omega_n^2$ and $k_d G = 2\zeta\omega_n$, then it is easy to verify that by setting

$$k_p = \underline{\omega_n}^2/\underline{G} \qquad k_d = 2\underline{\zeta}\underline{\omega_n}/\underline{G} \tag{59}$$

it occurs that $\zeta \geq \underline{\zeta}$ and $\omega_n \geq \underline{\omega_n}$ for all $\underline{G} \leq G \leq \overline{G}$. Since $G = l_c T_c / I$ then, clearly $\underline{G} = \underline{l_c}\ \underline{T_c}/\overline{I} = 1.13$ sec^{-2} and $\overline{G} = \overline{l_c}\ \overline{T_c}/\underline{I} = 4.05$ sec^{-2}. As a result, by Eq. (59) set $k_p = 0.43$ and $k_d = 0.99$.

The designed autopilot is first validated by analyzing the step response of system in Eq. (58) considering 20 values of G randomly uniformly distribuited between $\underline{G} = 1.13$ sec^{-2} and $\overline{G} = 4.05$ sec^{-2} (see Fig. 2). It turns out that for

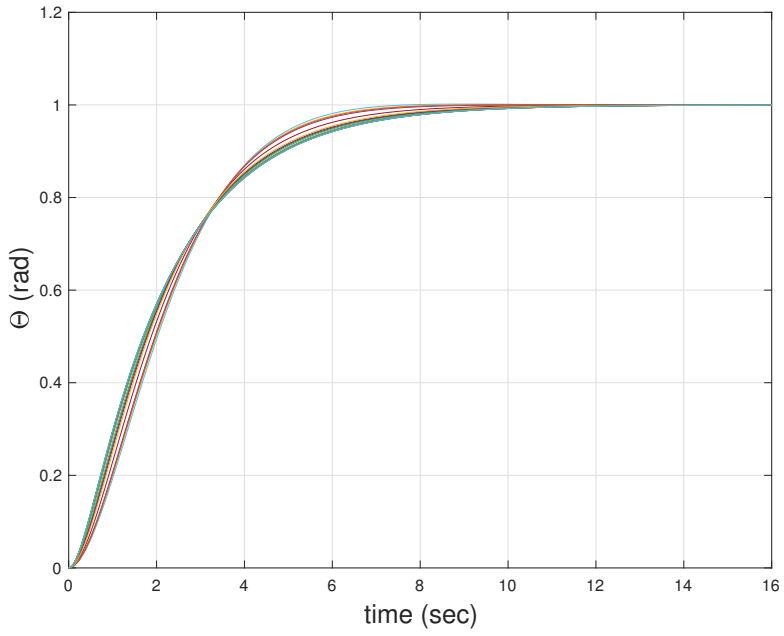

Figure 2: Step response of system in Eq. (58) for 20 random values of G.

all those 20 step responses it occurs that $M_p \leq 0.2\%$, 5.9 s $\leq t_s \leq$ 8.1 s, and 3.65 s $\leq t_r \leq$ 4.46 s. Thus, they all fulfill the specifications.

Moreover, theorem 1 is validated by simulating system in Eq. (9) with initial

state $[\widetilde{\Theta}(0)\ Q(0)]^T = [\widetilde{\Theta}_0\ Q_0]^T$ and constant parameter G selected as follows. Consider the following interval of variability

$$\mathcal{I}_1 = \Big\{[\widetilde{\Theta}_0\ Q_0\ G]|\ -180 \text{ deg} \leq \widetilde{\Theta}_0 \leq 180 \text{ deg},\ -0.1 \text{ rad/s} \leq Q_0 \leq 0.1 \text{ rad/s},$$
$$1.13 \text{ sec}^{-2} = \underline{G} \leq G \leq \overline{G} = 4.05 \text{ sec}^{-2}\Big\}$$

Then, 20 points randomly uniformly distributed over $\mathcal{I}_1$ have been selected. The corresponding time histories of $\widetilde{\Theta}$ and of $\text{sat}_{\overline{\Delta}}(\Delta)$ are plotted in Fig. 3. They

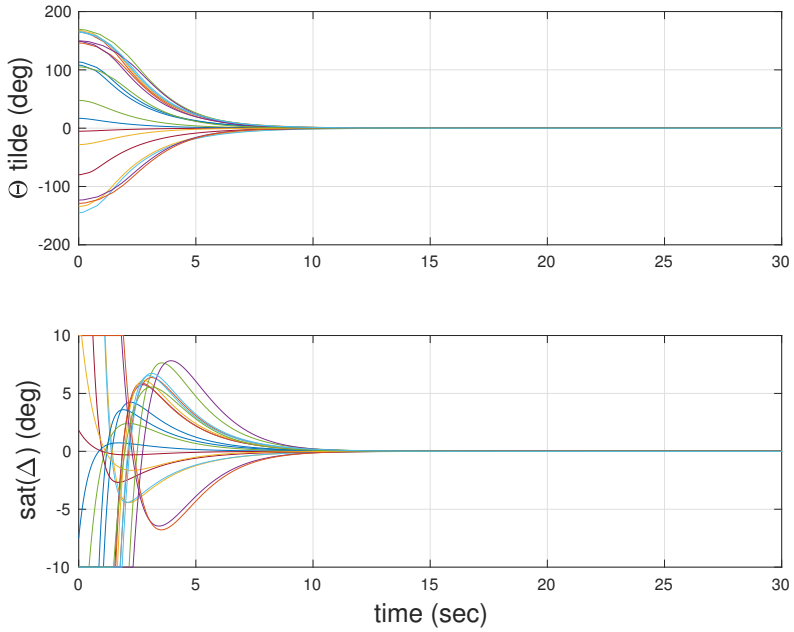

Figure 3: Time behaviors for 20 random values of $[\widetilde{\Theta}_0\ Q_0\ G]$ (design not including actuator).

confirm that equilibrium $[\widetilde{\Theta}\ Q]^T = [0\ 0]^T$ is robustly globally asymptotically stable. Note that the time behaviors of Θ can be obtained from those of $\widetilde{\Theta}$ through a simple translation since $\Theta = \widetilde{\Theta} + \Theta_c$.

The designed autopilot is then tested in the following more realistic scenario. Eqs. (3) and (4) controlled by PD autopilot in Eq. (8) are simulated considering the time-varying behaviors for l_c and I indicated in Eq.(56). The commanded-attitude Θ_c is also time-varying and represents a typical guidance command (see

Fig. 4). Thrust T_c is constant and uncertain. Consider the following interval of variability of initial state $[\Theta(0)\ Q(0)]^T = [\Theta_0\ Q_0]^T$ and of constant thrust T_c

$$\mathcal{I}_2 = \{[\Theta_0\ Q_0\ T_c] |\ -180 \text{ deg} \leq \Theta_0 \leq 180 \text{ deg},\ -0.1 \text{ rad/s} \leq Q_0 \leq 0.1 \text{ rad/s},$$
$$1.04 \cdot 10^4 \text{ N} = \underline{T_c} \leq T_c \leq \overline{T_c} = 1.27 \cdot 10^4 \text{ N}\}$$

Select 20 points randomly uniformly distributed over $\mathcal{I}_2$. The corresponding time histories of Θ and of $\text{sat}_{\overline{\Delta}}(\Delta)$ are plotted in Fig. 4.

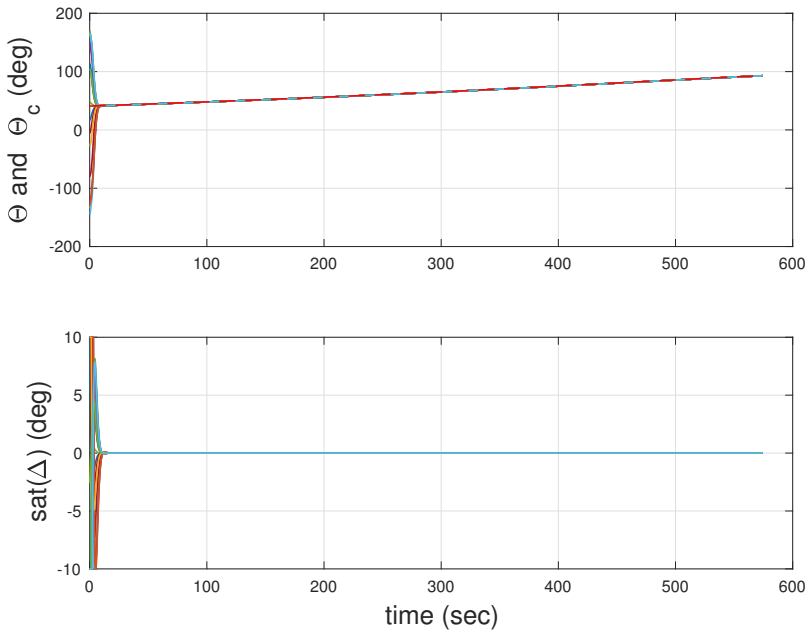

Figure 4: Time behaviors with time-varying Θ_c (red dashed line), l_c and I, and for 20 random values of $[\Theta_0\ Q_0\ T_c]$ (design not including actuator).

It is important to highlight that even when l_c, I, and Θ_c are time-varying, and consequently Proposition 1 does not apply, convergence of Θ to Θ_c is still attained. This occurs because the speeds of variation of l_c, I, and Θ_c are slow compared to the speed of convergence of Θ to Θ_c obtained when the latter are constant. Thus, in the time-varying scenario under consideration, those magnitudes act as if they were constant for the designed attitude control system.

The PD autopilot has been designed not taking into account of possible effects of the actuator. As a result, when simulations of the autopilot are performed including the model of the actuator in Eq. (6), if τ_a is much shorter than the minimum rise time $t_r \approx 3$ sec, then the time behaviors are close to the ones just obtained. However, for larger values of τ_a the performances of the PD autopilot deteriorate. For example with $\tau_a = 2.5$ sec, the time behaviors reported in Fig. 5 are obtained considering time-varying Θ_c, l_c, I as before, and setting $\Theta_0 = 0$, $Q_0 = 0$, $T_c = T_{c0} = 1.15 \cdot 10^4$ N. Clearly, instability occurs. Consequently, in such situations it is important to design an autopilot that takes

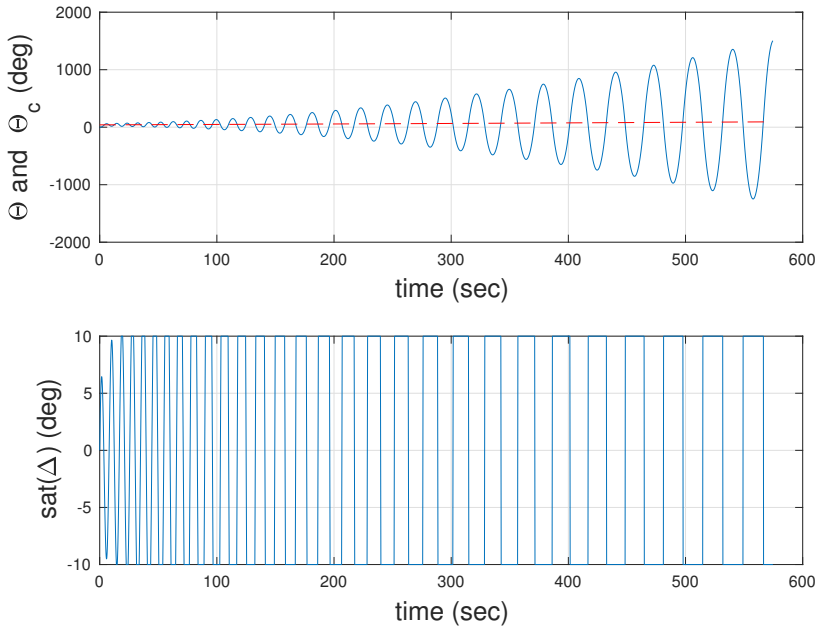

Figure 5: Time behaviors with time-varying Θ_c (red dashed line), l_c, I, and including actuator in simulation with $\tau_a = 2.5$ sec.

into account of the effects of the actuator. This is carried out in the following subsection

5.2. Autopilot Design Including the Dynamics of the Actuator.

In the present subsection autopilot design is performed using the same values and uncertainties for the parameters as in the previous subsection. However, here the model of the actuator in Eq. (6) is taken into account. It is set $\tau_a = 2.5$ sec as nominal value with a $\pm 10\%$ maximum uncertainty . Thus, 2.25 sec $= \underline{\tau_a} \leq \tau_a \leq \overline{\tau_a} = 2.75$ s. In subsection 4.3 it has been shown that a global robust autopilot is given by $\Delta_c = -\kappa(y)$ where $\kappa(y)$ is given by Eq. (54), y is given by Eq. (55), and σ is given by Eq. (35). The autopilot parameters have been determined as follows. The values $k_p = 0.43$ and $k_d = 0.99$ have been kept from the previous design. Gains $\underline{\kappa}_i \;\; i = 1, \ldots, 10$ have been determined by using the method described in subsection 4.3 leading to the following values $\underline{\kappa}_1 = 1.99 \cdot 10^{11}$, $\underline{\kappa}_2 = 1.58 \cdot 10^{21}$, $\underline{\kappa}_3 = 7.23 \cdot 10^{30}$, $\underline{\kappa}_4 = 7.71 \cdot 10^{40}$, $\underline{\kappa}_5 = 5.51 \cdot 10^{50}$, $\underline{\kappa}_6 = 2.84 \cdot 10^{60}$, $\underline{\kappa}_7 = 1.17 \cdot 10^{70}$, $\underline{\kappa}_8 = 3.90 \cdot 10^{79}$, $\underline{\kappa}_9 = 8.64 \cdot 10^{88}$, and $\underline{\kappa}_{10} = 1.08 \cdot 10^{98}$ [2].

To verify that the obtained controller stabilizes globally and robustly system in Eqs. (13)-(15), the corresponding closed-loop system has been simulated with constant G. The values for initial conditions $\widetilde{\Theta}(0) = \widetilde{\Theta}_0$ and $Q(0) = Q_0$, and for parameters G and τ_a have been picked as follows. Consider the following interval of variability

$$\mathcal{I}_3 = \Big\{ [\widetilde{\Theta}_0 \; Q_0 \; G \; \tau_a] | \; -180 \text{ deg} \leq \widetilde{\Theta}_0 \leq 180 \text{ deg},$$
$$-0.1 \text{ rad/s} \leq Q_0 \leq 0.1 \text{ rad/s}, \; 1.13 \text{ sec}^{-2} = \underline{G} \leq G \leq \overline{G} = 4.05 \text{ sec}^{-2},$$
$$2.25 \text{ sec} = \underline{\tau_a} \leq \tau_a \leq \overline{\tau_a} = 2.75 \text{ sec} \Big\}$$

Then, 20 points randomly uniformly distributed over $\mathcal{I}_3$ have been selected. The corresponding time histories of $\widetilde{\Theta}$ and of $\text{sat}_{\overline{\Delta}}(\Delta)$ are plotted in Fig. 6. Moreover, the global autopilot has been tested in the same time-varying scenario

[2] Such large gains might lead to numerical instability in the real engineering. However, since design of stabilizers by robust backstepping tends to be conservative, it is extremely likely that that much lower gains can be employed in practical applications. Investigating numerically the latter fact goes beyond the objective of the present work

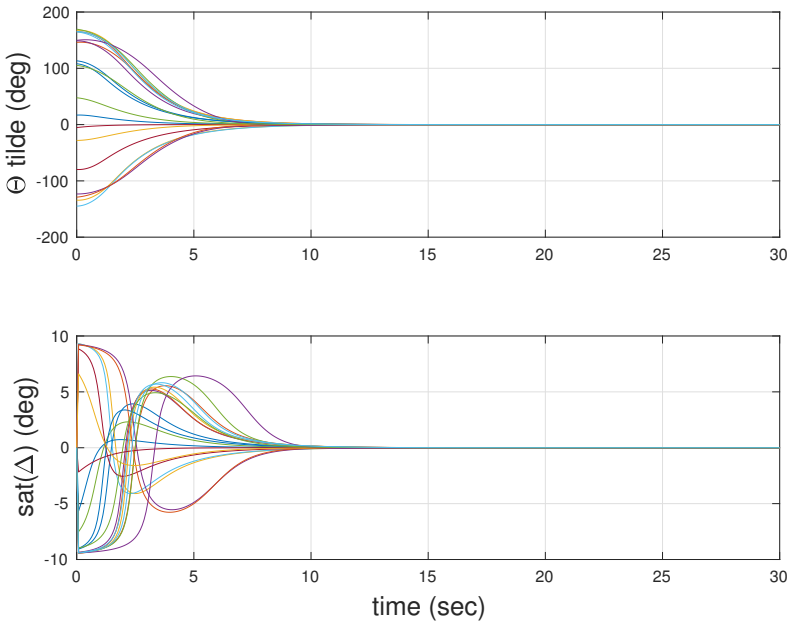

Figure 6: Time behaviors for 20 random values of $[\widetilde{\Theta}_0\ Q_0\ G\ \tau_a]$ (design including actuator).

as in subsection 5.1. Consider the following interval of variability of initial state $[\Theta(0)\ Q(0)]^T = [\Theta_0\ Q_0]^T$, constant thrust T_c, and time constant τ_a

$$\mathcal{I}_4 = \{[\Theta_0\ Q_0\ T_c\ \tau_a] |\ -180 \text{ deg} \le \Theta_0 \le 180 \text{ deg},$$
$$-0.1 \text{ rad/s} \le Q_0 \le 0.1 \text{ rad/s},\ 1.04 \cdot 10^4 \text{ N} = \underline{T_c} \le T_c \le \overline{T_c} = 1.27 \cdot 10^4 \text{ N},$$
$$2.25 \text{ sec} = \underline{\tau_a} \le \tau_a \le \overline{\tau_a} = 2.75 \text{ sec}\}$$

Then, 20 points randomly uniformly distributed over $\mathcal{I}_4$ have been selected. The corresponding time histories of Θ and of $\text{sat}_{\overline{\Delta}}(\Delta)$ are plotted in Fig. 7.

It is interesting to note that in Figs. 6 and 7 variable Δ never reaches it saturation limits $\pm\overline{\Delta} = \pm 10$ deg. The latter fact can be intuitively explained as follows. In equation (48) feedback $\Delta_c = -\kappa(y)$ with $\kappa(y)$ given by Eq. (54) is applied. The huge values of gains $\underline{\kappa_i}$ make variable y go to 0 very rapidly. Consequently, from Eq. (47) it follows that with the same speed Δ converges to $v^*(z)$. The latter fact guarantees that Δ never reaches saturation levels

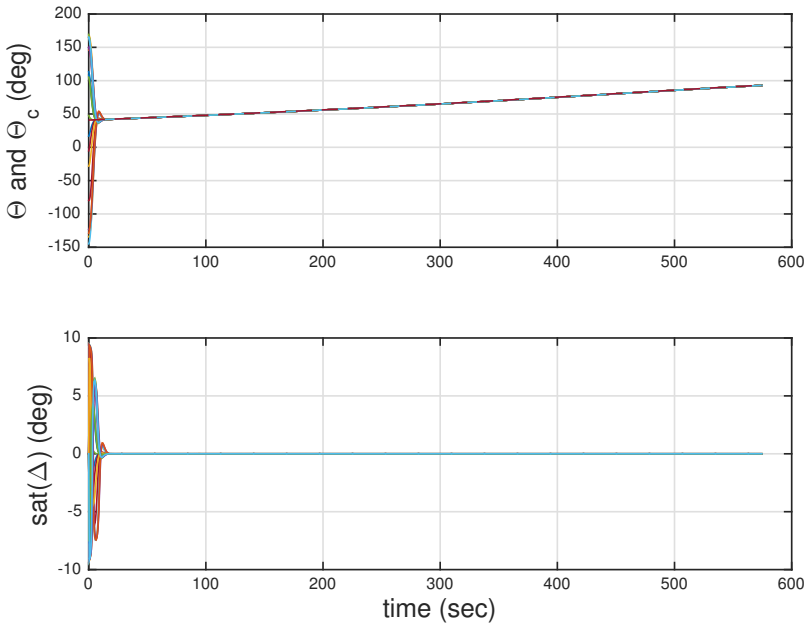

Figure 7: Time behaviors with time-varying Θ_c (red dashed line), l_c, I, and for 20 random values of $[\Theta_0\ Q_0\ T_c\ \tau_a]$ (design including actuator).

$\pm\overline{\Delta} = \pm 10$ deg (see Eqs. (34) and (35)).

5.3. Comparison with Adaptive PD Control

In this section the performances of the obtained autopilots are compared with those of an adaptive PD controller presented in [4].

The design of the adaptive PD controller employs the linearization of the model in Eq. (7) which is given by

$$\dot{x}_p = A_p x_p + B_b \Delta \tag{60}$$

where

$$x_p = \begin{bmatrix} \Theta \\ Q \end{bmatrix} \quad A_p = \begin{bmatrix} 0 & 1 \\ 0 & 0 \end{bmatrix} \quad B_p = \begin{bmatrix} 0 \\ G \end{bmatrix}$$

in which parameter $G = l_c T_c / I$ is subject to uncertainty. Next, the following

reference model is introduced

$$\dot{x}_m = A_m x_m + B_m \Theta_c$$

where

$$A_m = \begin{bmatrix} 0 & 1 \\ -\omega_m^2 & -2\zeta_m\, \omega_m \end{bmatrix} \quad B_m = \begin{bmatrix} 0 \\ \omega_m^2 \end{bmatrix}$$

The adaptive PD control law is given by

$$\Delta = -K_a(t)x + L_a(t)\Theta_c \tag{61}$$

where gains $K_a(t)$ and $L_a(t)$ are updated through the following equations (which are obtained from [4] after fixing some typos)

$$\dot{K}_a = e^T P B_m x^T \Gamma_K \qquad \dot{L}_a = -\Gamma_L \Theta_c B_m^T P e \tag{62}$$

In the previous equation $e = x - x_m$, and P is the solution to the following Lyapunov equation

$$P A_m + A_m^T P = -Q$$

in which Q is a symmetric positive definite matrix chosen by the designer. In Eq. (62) Γ_K denotes a symmetric positive definite matrix, and Γ_L is a positive scalar. Both Γ_K and Γ_L are design parameters. Paper [4] shows that the considered adaptive PD control guarantees that $\lim_{t\to\infty} e(t) = 0$.

The comparison between the autopilots obtained in this work and the considered adaptive PD controller, is carried out for the case study with the time-varying Θ_c, I and l_c previously introduced. Moreover thrust is set to its nominal value $T_c = T_{c0} = 1.15 \cdot 10^4$ N, and the initial conditions are chosen as $\Theta_0 = 0$, $Q_0 = 0$.

The design parameters for the adaptive PD control have been selected as follows. The parameters of the reference model have been set as $\zeta_m = 0.8$ and $\omega_m = 0.7$ rad/s. In fact, those values guarantee that the reference model fulfills the previously introduced specifications $M_p \leq 2\%$, $t_s \leq 10$ sec, $t_r \leq 5$ sec (see subsection 5.1). Moreover, it has been set $Q = I_{2\times 2}$, and proceeding by trial and error, gains Γ_K and Γ_L have been selected as $\Gamma_K = 10 I_{2\times 2}$, $\Gamma_L = 10$.

The initial values for the adaptive gains K_a and L_a have bee chosen as follows. Consider the value of G at time $t = 0$ which is given by $G_0 = l_{ci}T_{c0}/I_i$. Then $K_a(0)$ and $L_a(0)$ have been determined enforcing that the closed-loop system in Eqs. (60)-(61) considered at time $t = 0$, coincides with the reference model. The resulting values are $K_a(0) = [\omega_m^2/G_0 \; 2\zeta_m \; \omega_m/G_0]$, $L_a(0) = \omega_m^2/G_0$

Several simulations have been executed using different values for the time constant of the electro-hydraulic servoactuator τ_a. Note that the design of the adaptive PD control has been performed not considering the effects of the actuator as it was done with the PD control designed in subsection 5.1. Thus, initially it has been set $\tau_a = 0$. The resulting time histories of Θ reported in Fig. 8 show that both controllers are able to track Θ_c. However, a slightly better

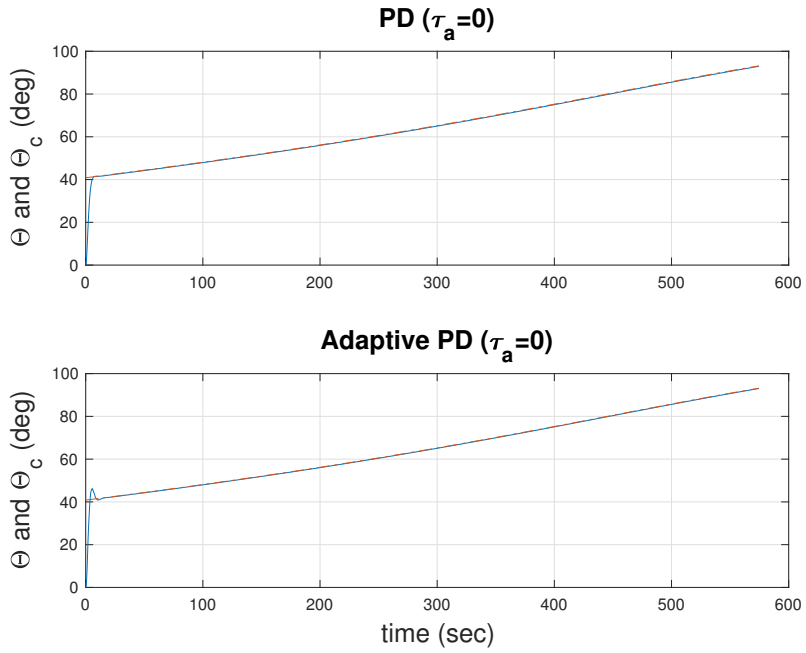

Figure 8: Time behaviors with time-varying Θ_c (red dashed line), l_c, I, using PD control and adaptive PD control with $\tau_a = 0$.

response is obtained with PD control since it does not exhibit overshoot.

Next, PD control and adaptive PD control are compared when the vehicle

model includes an actuator having $\tau_a = 0.3$ sec . The corresponding time histories of Θ reported in Fig. 9 show that the transient behavior with adaptive PD is substantially worse than with PD control.

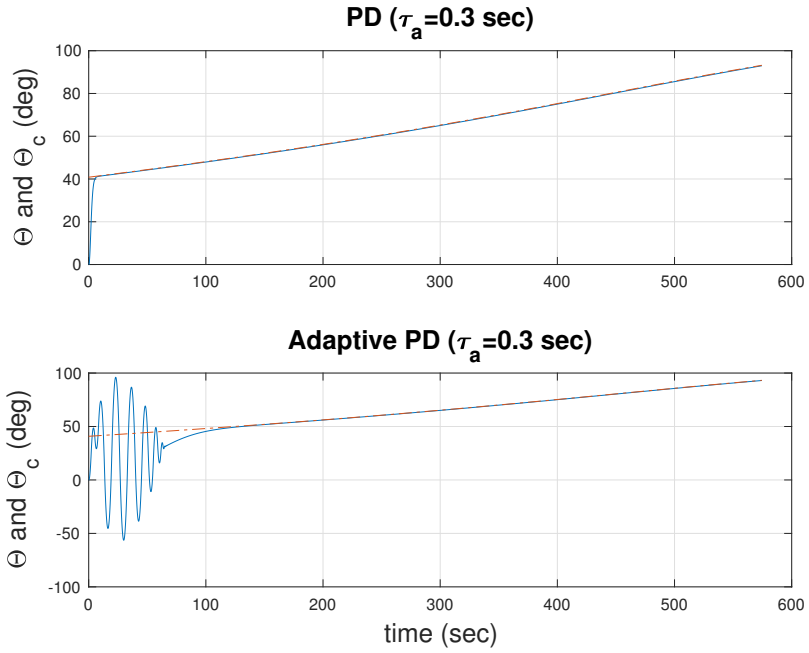

Figure 9: Time behaviors with time-varying Θ_c (red dashed line), l_c, I, using PD control and adaptive PD control with $\tau_a = 0.3$ sec.

Finally, an actuator with $\tau_a = 2.5$ sec is considered. It has been already shown that this leads PD control to instability (see Fig. 5). Moreover, Fig. 10 shows that the same happens with adaptive PD. On the other hand, the same figure confirms that using the robust backstepping autopilot from subsection 5.2, makes Θ track the guidance command Θ_c.

In conclusion, the comparison shows that if the actuator is fast with respect to the attitude control loop, then both PD and adaptive PD are effective. However, PD control performs better in terms of quality of the transient response. For slow actuators both PD and adaptive PD lead to instability, whereas robust backstepping control achieves good tracking performance.

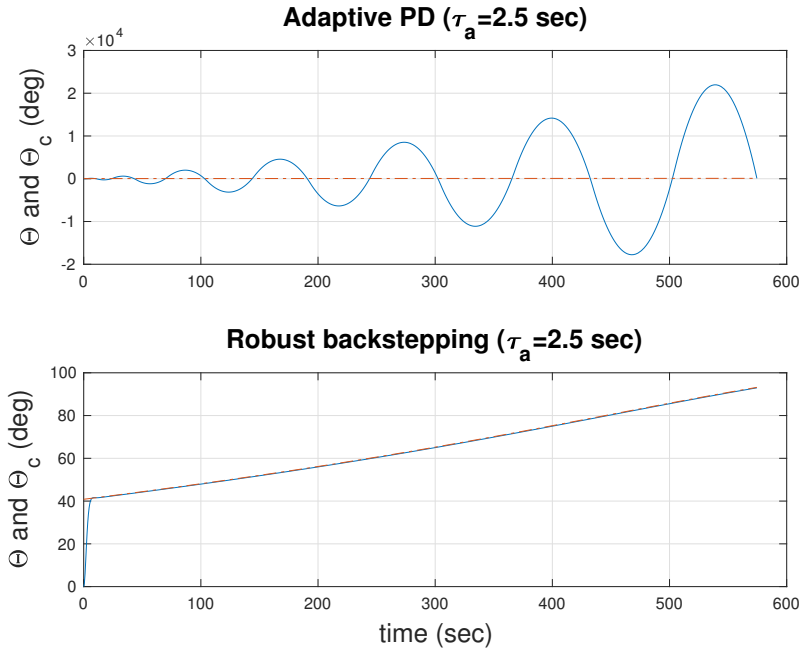

Figure 10: Time behaviors with time-varying Θ_c (red dashed line), l_c, I, using adaptive PD and robust backstepping with $\tau_a = 2.5$ sec.

6. Conclusions

In the present paper two autopilots have been designed based on a nonlinear model of a rigid launch vehicle flying a planar trajectory above atmosphere. Both autopilots possess the interesting feature of guaranteeing global convergence even considering parametric uncertainties. Global convergence is important because when large angle maneuvers must be performed, it is simpler to use a single global controller than several local controllers patched together. The effectiveness of the obtained autopilots is shown through a case study.

Acknowledgement

The author acknowledges Prof. P. Teofilatto for fruitful discussions and Dr. Dennis Lucarelli for his help.

Appendix A. Determination of $\underline{\alpha}^\circ$ and $\overline{\alpha}^\circ$

The first goal of the present appendix is determining $\underline{\alpha}^\circ \in \mathcal{K}_\infty$ such that

$$V^\circ(z,G) \triangleq G(\Phi(k_p\Theta) + \Phi(k_p\Theta + k_d Q)) + k_p Q^2 \geq \underline{\alpha}^\circ(\|z\|) \qquad \forall z \in \mathbb{R}^2 \;\; \forall G \in [\underline{G}\ \overline{G}] \quad \text{(A.1)}$$

First note that since Φ is a nonnegative and even function, the following holds

$$V^\circ(z,G) \geq \underline{G}\Phi(k_p|\Theta|) + k_p Q^2 \quad \forall z \in \mathbb{R}^2 \;\; \forall G \in [\underline{G}\ \overline{G}] \quad \text{(A.2)}$$

The next intermediate objective is finding $\epsilon \in \mathcal{K}_\infty$ that fulfills $\Phi(r) \geq \epsilon(r)$ and $r^2 \geq \epsilon(r)$ for all $r \geq 0$. For that purpose note that

$$\Phi''(r) = \sigma'(r) = \frac{1}{1 + \left(\frac{\pi}{2\sin\overline{\Delta}} r\right)^2} \quad \text{(A.3)}$$

thus $\Phi''(r)$ is strictly decreasing for $r \geq 0$. Moreover, since $\Phi''(\frac{2\sin\overline{\Delta}}{\pi}) = 1/2$, then

$$\Phi''(r) \geq \epsilon_1(r) \;\; \forall r \geq 0 \quad \text{(A.4)}$$

where

$$\epsilon_1(r) \triangleq \begin{cases} \frac{1}{2} & \text{if } 0 \leq r \leq \frac{2\sin\overline{\Delta}}{\pi} \\ 0 & \text{if } r > \frac{2\sin\overline{\Delta}}{\pi} \end{cases}$$

Integrating Eq. (A.4) over the interval $[0\ r]$ obtain

$$\Phi'(r) \geq \epsilon_2(r) \;\; \forall r \geq 0 \quad \text{(A.5)}$$

where

$$\epsilon_2(r) \triangleq \begin{cases} \frac{1}{2} r & \text{if } 0 \leq r \leq \frac{2\sin\overline{\Delta}}{\pi} \\ \frac{\sin\overline{\Delta}}{\pi} & \text{if } r > \frac{2\sin\overline{\Delta}}{\pi} \end{cases}$$

Thus, integration Eq. (A.5) over the interval $[0\ r]$ leads to $\Phi(r) \geq \epsilon(r)$ for all $r \geq 0$ where ϵ is the following class $\mathcal{K}_\infty$ function

$$\epsilon(r) \triangleq \begin{cases} \frac{1}{4} r^2 & \text{if } 0 \leq r \leq \frac{2\sin\overline{\Delta}}{\pi} \\ \frac{\sin^2\overline{\Delta}}{\pi^2} + \frac{\sin\overline{\Delta}}{\pi}\left(r - \frac{2\sin\overline{\Delta}}{\pi}\right) & \text{if } r > \frac{2\sin\overline{\Delta}}{\pi} \end{cases}$$

Clearly $r^2 \geq \epsilon(r)$ for all $r \geq 0$. Thus, from Eq. (A.2) obtain

$$V^\circ(z,G) \geq \underline{G}\epsilon(k_p|\Theta|) + k_p\epsilon(|Q|) \quad \forall z \in \mathbb{R}^2 \;\; \forall G \in [\underline{G}\;\overline{G}]$$

Let $a \triangleq \min\{\underline{G}, k_p\}$. By using a property of class $\mathcal{K}_\infty$ functions reported on p. 188 of [15] obtain

$$V^\circ(z,G) \geq a(\epsilon(k_p|\Theta|) + \epsilon(|Q|)) \geq a\epsilon\left(\frac{1}{2}k_p|\Theta| + \frac{1}{2}|Q|\right) \quad \forall z \in \mathbb{R}^2 \;\; \forall G \in [\underline{G}\;\overline{G}]$$

Let $b \triangleq \min\{1, k_p\}$, then

$$V^\circ(z,G) \geq a\epsilon\left(\frac{1}{2}b(|\Theta| + |Q|)\right) \geq a\epsilon\left(\frac{1}{2}b\|z\|\right) = \underline{\underline{\alpha}}^\circ(\|z\|)$$
$$\forall z \in \mathbb{R}^2 \;\; \forall G \in [\underline{G}\;\overline{G}] \quad \text{(A.6)}$$

where $\underline{\underline{\alpha}}^\circ(r) \triangleq a\epsilon\left(\frac{1}{2}br\right)$ can be equivalently rewritten as

$$\underline{\underline{\alpha}}^\circ(r) = \begin{cases} \underline{\underline{\alpha}}_0^\circ r^2 & \text{if } 0 \leq r \leq r^* \\ \underline{\underline{\alpha}}_0^\circ (r^*)^2 + \underline{\underline{\alpha}}_1^\circ (r - r^*) & \text{if } r > r^* \end{cases}$$

with $\underline{\underline{\alpha}}_0^\circ \triangleq ab^2/16$, $\underline{\underline{\alpha}}_1^\circ \triangleq ab\sin\overline{\Delta}/(2\pi)$, and $r^* \triangleq 4\sin\overline{\Delta}/(\pi b)$. Introduce the following class $\mathcal{K}_\infty$ function

$$\underline{\alpha}^\circ(r) \triangleq \underline{\alpha}_0^\circ r^2/(1 + \underline{\alpha}_1^\circ r) \quad \text{(A.7)}$$

where $\underline{\alpha}_0^\circ \triangleq \underline{\underline{\alpha}}_0^\circ/2$ and $\underline{\alpha}_1^\circ \triangleq \underline{\underline{\alpha}}_0^\circ/\underline{\underline{\alpha}}_1^\circ$. Next, it will be shown that

$$\underline{\underline{\alpha}}^\circ(r) \geq \underline{\alpha}^\circ(r) \quad \forall r \geq 0 \quad \text{(A.8)}$$

In fact, for $0 \leq r \leq r^*$ the following holds $\underline{\underline{\alpha}}^\circ(r) \geq \underline{\underline{\alpha}}_0^\circ r^2/2 = \underline{\alpha}_0^\circ r^2 \geq \underline{\alpha}^\circ(r)$. For showing that $\underline{\underline{\alpha}}^\circ(r) \geq \underline{\alpha}^\circ(r)$ for $r > r^*$ proceed as follows. First note that $\underline{\underline{\alpha}}^\circ(r^*) > \underline{\alpha}^\circ(r^*)$; in fact

$$\underline{\underline{\alpha}}^\circ(r^*) = \underline{\underline{\alpha}}_0^\circ(r^*)^2 > \frac{1}{2}\underline{\underline{\alpha}}_0^\circ(r^*)^2 > \frac{\frac{1}{2}\underline{\underline{\alpha}}_0^\circ(r^*)^2}{1 + \frac{\underline{\underline{\alpha}}_0^\circ}{\underline{\underline{\alpha}}_1^\circ}r^*} = \underline{\alpha}^\circ(r^*)$$

Moreover, through standard computations it can be shown that $(\underline{\underline{\alpha}}^\circ)'(r) > (\underline{\alpha}^\circ)'(r)$ for all $r > r^*$. Thus, it has been proved that Eq. (A.8) holds. Consequently, by Eq. (A.6) obtain that the class $\mathcal{K}_\infty$ function $\underline{\alpha}^\circ$ defined in Eq. (A.7), fulfills Eq. (A.1).

The second objective of the present appendix is determining $\overline{\alpha}^{\circ} \in \mathcal{K}_{\infty}$ such that

$$V^{\circ}(z,G) \triangleq G(\Phi(k_p\Theta) + \Phi(k_p\Theta + k_dQ)) + k_pQ^2 \leq \overline{\alpha}^{\circ}(\|z\|) \qquad \forall z \in \mathbb{R}^2 \;\; \forall G \in [\underline{G}\;\overline{G}] \quad \text{(A.9)}$$

First note that since $\Phi(r)$ is strictly increasing for $r \geq 0$ and is an even function, then the following holds

$$V^{\circ}(z,G) \leq \overline{G}(\Phi(k_p|\Theta|) + \Phi(k_p|\Theta| + k_d|Q|)) + k_pQ^2 \quad \forall z \in \mathbb{R}^2 \;\; \forall G \in [\underline{G}\;\overline{G}]$$

Next, since $\sigma(r) \leq r$ for $r \geq 0$, it holds that $\Phi(r) \leq r^2/2$ for $r \geq 0$. Thus, by using the latter property as well as inequality $|\Theta||Q| \leq \Theta^2/2 + Q^2/2$, it is easy to obtain that Eq. (A.9) is fulfilled with $\overline{\alpha}^{\circ}(r) = \overline{\alpha}_0^{\circ} r^2$ where

$$\overline{\alpha}_0^{\circ} = \max\left\{\overline{G}k_p\left(k_p + \frac{1}{2}k_d\right), \frac{1}{2}\overline{G}k_d\left(k_p + k_d\right) + k_p\right\}$$

Appendix B. Determination of $\boldsymbol{\alpha}^{\circ}$

Let

$$W_0(z,G) \triangleq -\frac{\partial V^{\circ}}{\partial z}(z,G) f_z(z, v^*(z), G) = Gk_pQ(\sigma(k_p\widetilde{\Theta} + k_dQ) - \sigma(k_p\widetilde{\Theta})) + G^2k_d\sigma^2(k_p\widetilde{\Theta} + k_dQ)$$

The purpose of the current subsection is determining $\alpha^{\circ} \in \mathcal{K}$ such that

$$W_0(z,G) \geq \alpha^{\circ}(\|z\|) \quad \forall z \in \mathbb{R}^2 \;\; \forall G \in [\underline{G}\;\overline{G}] \qquad \text{(B.1)}$$

Let

$$W_1(z) \triangleq \underline{G}k_pQ(\sigma(k_p\widetilde{\Theta} + k_dQ) - \sigma(k_p\widetilde{\Theta})) + \underline{G}^2k_d\sigma^2(k_p\widetilde{\Theta} + k_dQ) \qquad \text{(B.2)}$$

Since terms $Q(\sigma(k_p\widetilde{\Theta} + k_dQ) - \sigma(k_p\widetilde{\Theta}))$ and $\sigma^2(k_p\widetilde{\Theta} + k_dQ)$ are nonnegative, then clearly

$$W_0(z,G) \geq W_1(z) \quad \forall z \in \mathbb{R}^2 \;\; \forall G \in [\underline{G}\;\overline{G}] \qquad \text{(B.3)}$$

Then, in order to find $\alpha^\circ \in \mathcal{K}$ such that $W_1(z) \geq \alpha^\circ(\|z\|)$ for all $z \in \mathbb{R}^2$, the following approach, inspired by remark 10.1.3 of [17], will be followed. Given $c \geq 0$ consider the level set $\Omega_c \triangleq \{z \in \mathbb{R}^2 : W_1(z) \leq c\}$. Given an appropriate $\bar{c} > 0$ that will be determined later, find a continuous strictly increasing function $\rho : [0\ \bar{c}) \to [0\ \infty)$ such that $\rho(0) = 0$, $\lim_{r \to \bar{c}^-} \rho(r) = \infty$, and such that it possesses the following property

$$z \in \Omega_c \Rightarrow \|z\| \leq \rho(c) \tag{B.4}$$

The latter property means that for $0 \leq c < \bar{c}$, the disk of radius $\rho(c)$ contains the level set Ω_c. Then, consider the inverse function $\rho^{-1} : [0\ \infty) \to [0\ \bar{c})$ and note that $\rho^{-1} \in \mathcal{K}$. It occurs that

$$W_1(z) \geq \rho^{-1}(\|z\|) \quad \forall z \in \mathbb{R}^2 \tag{B.5}$$

In fact, pick a generic $z \in \mathbb{R}^2$, and let $c = W_1(z)$; then, clearly $z \in \Omega_c$. If $c < \bar{c}$, then by Eq. (B.4) obtain that $\|z\| \leq \rho(c) = \rho(W_1(z))$. Consequently $W_1(z) \geq \rho^{-1}(\|z\|)$. On the other hand, if $c \geq \bar{c}$ then $W_1(z) = c \geq \bar{c} > \rho^{-1}(\|z\|)$. Consequently, Eq. (B.5) holds true, and by Eq. (B.3), setting

$$\alpha^\circ(r) = \rho^{-1}(r) \qquad r \geq 0 \tag{B.6}$$

it follows that Eq. (B.1) is fulfilled.

Thus, the next step is finding an explicit expression for $\rho^{-1}(r)$. For that purpose, it is important to determine a function ρ that satisfies the properties previously indicated and for which it is possible to compute explicitly the inverse function. Then, starting from Eq. (B.2), note that by the mean value theorem

$$\sigma(k_p\widetilde{\Theta} + k_dQ) - \sigma(k_p\widetilde{\Theta}) = \sigma'(\xi)k_dQ$$
$$\min\{k_p\widetilde{\Theta} + k_dQ, k_p\widetilde{\Theta}\} < \xi < \max\{k_p\widetilde{\Theta} + k_dQ, k_p\widetilde{\Theta}\}$$

Since σ' is even then

$$\sigma(k_p\widetilde{\Theta} + k_dQ) - \sigma(k_p\widetilde{\Theta}) = \sigma'(|\xi|)k_dQ \quad |\xi| < k_p|\widetilde{\Theta}| + k_d|Q|,$$

Moreover, since also σ^2 is even, then $\sigma^2(k_p\widetilde{\Theta}+k_dQ)=\sigma^2(|k_p\widetilde{\Theta}+k_dQ|)$. Thus

$$W_1(z)=\underline{G}k_pk_d\sigma'(|\xi|)Q^2+\underline{G}^2k_d\sigma^2(|k_p\widetilde{\Theta}+k_dQ|)\quad |\xi|<k_p|\widetilde{\Theta}|+k_d|Q| \tag{B.7}$$

Pick $0\leq c<c^*$ where c^* will be determined later. Then, $z\in\Omega_c$ implies

$$\sigma^2(|k_p\widetilde{\Theta}+k_dQ|)\leq\frac{1}{\underline{G}^2k_d}c \tag{B.8}$$

Note that the range of σ^2 is equal to $[0\ \sin^2\overline{\Delta})$. Then, c^* will be picked such that

$$c^*<\underline{G}^2k_d\sin^2\overline{\Delta} \tag{B.9}$$

so that the right-hand side of Eq. (B.8) is smaller than $\sin^2\overline{\Delta}$. Denote by $\tau:[0\ \sin^2\overline{\Delta})\to[0\ \infty)$ the inverse function of σ^2 restricted to the interval $[0\ \infty)$. It easy to show that

$$\tau(r)=\frac{2\sin\overline{\Delta}}{\pi}\tan\left(\frac{\pi}{2\sin\overline{\Delta}}\sqrt{r}\right)$$

Consequently Eq. (B.8) implies

$$|k_p\widetilde{\Theta}+k_dQ|\leq\tau\left(\frac{1}{\underline{G}^2k_d}c\right)$$

Since $k_p|\widetilde{\Theta}|-k_d|Q|\leq|k_p\widetilde{\Theta}+k_dQ|$, then from the equation above obtain

$$k_p|\widetilde{\Theta}|\leq k_d|Q|+\tau\left(\frac{1}{\underline{G}^2k_d}c\right) \tag{B.10}$$

Thus, it has been obtained so far that if $z\in\Omega_c$ with $0\leq c<c^*$, then the above inequality holds. As a result, for all such z's Eq. (B.7) can be rewritten as follows

$$W_1(z)=\underline{G}k_pk_d\sigma'(|\xi|)k_dQ^2+\underline{G}^2k_d\sigma^2(|k_p\widetilde{\Theta}+k_dQ|)\quad |\xi|<2k_d|Q|+\tau\left(\frac{1}{\underline{G}^2k_d}c\right)$$

Then, $z\in\Omega_c$ with $0\leq c<c^*$ implies

$$\underline{G}k_pk_d\sigma'(|\xi|)Q^2\leq c\quad\text{ with }\quad|\xi|<2k_d|Q|+\tau\left(\frac{1}{\underline{G}^2k_d}c\right)$$

Using the expression in Eq. (A.3) for σ' obtain

$$\underline{G}k_pk_dQ^2\leq c\left(1+\frac{\pi^2}{4\sin^2\overline{\Delta}}\xi^2\right)\quad\text{ with }\quad|\xi|<2k_d|Q|+\tau\left(\frac{1}{\underline{G}^2k_d}c\right)$$

which implies

$$\left(\underline{G}k_pk_d - c\frac{\pi^2k_d^2}{\sin^2\overline{\Delta}}\right)Q^2 - c\frac{\pi^2k_d}{\sin^2\overline{\Delta}}\tau\left(\frac{1}{\underline{G}^2k_d}c\right)|Q| - c\left(1+\left(\frac{\pi}{2\sin\overline{\Delta}}\tau\left(\frac{1}{\underline{G}^2k_d}c\right)\right)^2\right) \leq 0 \quad \text{(B.11)}$$

Then c^* will be picked such that

$$c^* < \frac{\underline{G}k_p\sin^2\overline{\Delta}}{\pi^2k_d}$$

In fact, since $0 \leq c < c^*$, the latter choice guarantees the positivity of the term multiplying Q^2 in Eq. (B.11). Thus, taking into account also of Eq. (B.9), set

$$c^* = \frac{1}{2}\min\left\{\underline{G}^2k_d\sin^2\overline{\Delta}\ ,\ \frac{\underline{G}k_p\sin^2\overline{\Delta}}{\pi^2k_d}\right\}$$

Then, Eq. (B.11) implies that for $z \in \Omega_c$ with $0 \leq c < c^*$ the following holds

$$\begin{aligned}
|Q| &\leq \frac{c\frac{\pi^2k_d}{\sin^2\overline{\Delta}}\tau\left(\frac{1}{\underline{G}^2k_d}c\right)}{2\left(\underline{G}k_pk_d - c\frac{\pi^2k_d^2}{\sin^2\overline{\Delta}}\right)} \\
&+ \frac{\sqrt{\left(c\frac{\pi^2k_d}{\sin^2\overline{\Delta}}\tau\left(\frac{1}{\underline{G}^2k_d}c\right)\right)^2 + 4\left(\underline{G}k_pk_d - c\frac{\pi^2k_d^2}{\sin^2\overline{\Delta}}\right)c\left(1+\left(\frac{\pi}{2\sin\overline{\Delta}}\tau\left(\frac{1}{\underline{G}^2k_d}c\right)\right)^2\right)}}{2\left(\underline{G}k_pk_d - c\frac{\pi^2k_d^2}{\sin^2\overline{\Delta}}\right)} \\
&\leq \frac{c\frac{\pi^2k_d}{\sin^2\overline{\Delta}}\tau\left(\frac{1}{\underline{G}^2k_d}c\right)}{2\underline{G}k_pk_d\left(1 - c\frac{\pi^2k_d}{\underline{G}k_p\sin^2\overline{\Delta}}\right)} \\
&+ \frac{\sqrt{c^2\left(\frac{\pi^2k_d}{\sin^2\overline{\Delta}}\tau\left(\frac{1}{\underline{G}^2k_d}c\right)\right)^2 + 4\underline{G}k_pk_dc\left(1+\left(\frac{\pi}{2\sin\overline{\Delta}}\tau\left(\frac{1}{\underline{G}^2k_d}c\right)\right)^2\right)}}{2\underline{G}k_pk_d\left(1 - c\frac{\pi^2k_d}{\underline{G}k_p\sin^2\overline{\Delta}}\right)} \\
&\leq \frac{\sqrt{c^*}\frac{\pi^2k_d}{\sin^2\overline{\Delta}}\tau\left(\frac{1}{\underline{G}^2k_d}c^*\right)\sqrt{c}}{2\underline{G}k_pk_d\left(1 - \frac{c}{c^*}\right)} \\
&+ \frac{\sqrt{\left(c^*\left(\frac{\pi^2k_d}{\sin^2\overline{\Delta}}\tau\left(\frac{1}{\underline{G}^2k_d}c^*\right)\right)^2 + 4\underline{G}k_pk_d\left(1+\left(\frac{\pi}{2\sin\overline{\Delta}}\tau\left(\frac{1}{\underline{G}^2k_d}c^*\right)\right)^2\right)\right)c}}{2\underline{G}k_pk_d\left(1 - \frac{c}{c^*}\right)}
\end{aligned} \quad \text{(B.12)}$$

Note that the term $\tau\left(\frac{1}{\underline{G}^2 k_d} c^*\right)$ is bounded since

$$\tau\left(\frac{1}{\underline{G}^2 k_d} c^*\right) \leq \tau\left(\frac{\sin^2 \overline{\Delta}}{2}\right) = \frac{2 \sin \overline{\Delta}}{\pi} \tan\left(\frac{\pi}{2\sqrt{2}}\right)$$

For $0 \leq c < c^*$ define

$$\rho_1(c) \triangleq \rho_1^\circ \frac{\sqrt{c}}{1 - \frac{c}{c^*}}$$

with

$$\rho_1^\circ \triangleq \frac{\sqrt{c^*} \frac{\pi^2 k_d}{\sin^2 \overline{\Delta}} \tau\left(\frac{1}{\underline{G}^2 k_d} c^*\right)}{2\underline{G} k_p k_d} + \frac{\sqrt{c^* \left(\frac{\pi^2 k_d}{\sin^2 \overline{\Delta}} \tau\left(\frac{1}{\underline{G}^2 k_d} c^*\right)\right)^2 + 4\underline{G} k_p k_d \left(1 + \left(\frac{\pi}{2 \sin \overline{\Delta}} \tau\left(\frac{1}{\underline{G}^2 k_d} c^*\right)\right)^2\right)}}{2\underline{G} k_p k_d}$$

Then, from Eq. (B.12) obtain that for $z \in \Omega_c$ with $0 \leq c < c^*$ it occurs that $|Q| \leq \rho_1(c)$. It is easy to verify that

$$\frac{1}{1 - \frac{1}{c^*} c} \leq \frac{1}{\left(1 - \frac{2}{c^*} c\right)^{1/2}} \quad \forall c \in [0 \ c^*/2)$$

Thus, letting $\bar{c} \triangleq c^*/2$, obtain that for $z \in \Omega_c$ with $0 \leq c < \bar{c}$, it occurs that

$$|Q| \leq \rho_2(c) \tag{B.13}$$

where

$$\rho_2(c) \triangleq \rho_1^\circ \left(\frac{c}{1 - \frac{c}{\bar{c}}}\right)^{1/2} \tag{B.14}$$

Using Eqs. (B.10) and (B.13) obtain that $z \in \Omega_c$ with $0 \leq c < \bar{c}$ implies

$$|\widetilde{\Theta}| \leq \frac{k_d}{k_p} \rho_2(c) + \frac{1}{k_p} \tau\left(\frac{1}{\underline{G}^2 k_d} c\right)$$

Then, combining Eq. (B.13) and the equation above, it follows that $z \in \Omega_c$ with $0 \leq c < \bar{c}$ implies

$$\|z\| \leq |\widetilde{\Theta}| + |Q| \leq \left(\frac{k_d}{k_p} + 1\right) \rho_2(c) + \frac{1}{k_p} \tau\left(\frac{1}{\underline{G}^2 k_d} c\right) \tag{B.15}$$

In order to obtain an upper bound for $\|z\|$ as function of c for which it is possible to compute analytically the inverse function, proceed as follows. By using the following inequality

$$\tan(x) \leq \frac{1}{\cos^2(\bar{x})} x \qquad 0 \leq x < \bar{x} < \frac{\pi}{2}$$

obtain

$$\tau\left(\frac{1}{\underline{G}^2 k_d}c\right) = \frac{2\sin\overline{\Delta}}{\pi}\tan\left(\frac{\pi}{2\underline{G}\sqrt{k_d}\sin\overline{\Delta}}\sqrt{c}\right)$$
$$\leq \frac{1}{\underline{G}\sqrt{k_d}\cos^2\left(\frac{\pi}{2\underline{G}\sqrt{k_d}\sin\overline{\Delta}}\sqrt{\bar{c}}\right)}\sqrt{c} \quad \forall c \in [0\ \bar{c}) \quad \text{(B.16)}$$

Moreover, clearly the following holds

$$\sqrt{c} \leq \left(\frac{c}{1-\frac{c}{\bar{c}}}\right)^{1/2} \quad \forall c \in [0\ \bar{c}) \quad \text{(B.17)}$$

Thus, from Eqs. (B.14) - (B.17) obtain that if $z \in \Omega_c$ with $0 \leq c < \bar{c}$, then $\|z\| \leq \rho(c)$ where

$$\rho(c) \triangleq \rho^\circ\left(\frac{c}{1-\frac{c}{\bar{c}}}\right)^{1/2}$$

and

$$\rho^\circ = \left(\frac{k_d}{k_p}+1\right)\rho_1^\circ + \frac{1}{\underline{G}\sqrt{k_d^3}\cos^2\left(\frac{\pi}{2\underline{G}\sqrt{k_d}\sin\overline{\Delta}}\sqrt{\bar{c}}\right)}$$

The inverse function of ρ can be computed analytically. Thus, from Eq. (B.6) the following holds

$$\alpha^\circ(r) = \rho^{-1}(r) = \frac{\alpha_0^\circ r^2}{1+\alpha_1^\circ r^2}$$

with $\alpha_0^\circ = 1/(\rho^\circ)^2$ and $\alpha_1^\circ = 1/((\rho^\circ)^2\bar{c})$.

Appendix C. Determination of $\widehat{\alpha}$.

The purpose of the current appendix is determining $\widehat{\alpha}$ such that Eq. (42) holds. From Eqs. (37) and (41) obtain

$$\left|\frac{\partial V_z}{\partial Q}(z,G)\right| \leq V^\circ(z,G)\left|\frac{\partial V^\circ}{\partial Q}(z,G)\right| \leq \overline{\alpha}^\circ(\|z\|)\left|\frac{\partial V^\circ}{\partial Q}(z,G)\right|$$
$$\forall z \in \mathbb{R}^2 \ \ \forall G \in [\underline{G}\ \overline{G}] \quad \text{(C.1)}$$

Eq. (36) leads to

$$\left|\frac{\partial V^\circ}{\partial Q}(z,G)\right| \leq \overline{G}k_d\sigma(k_p|\widetilde{\Theta}| + k_d|Q|) + 2k_p|Q| \leq \sqrt{2}d\|z\|$$
$$\forall z \in \mathbb{R}^2 \ \ \forall G \in [\underline{G}\ \overline{G}] \quad \text{(C.2)}$$

with $d \triangleq \max\{\overline{G}k_pk_d, \overline{G}k_d^2 + 2k_p\}$. Thus, using Eqs. (38) and (C.1), obtain Eq. (42) with $\widehat{\alpha}(r) = \widehat{\alpha}_0 r^3$ where $\widehat{\alpha}_0 = \sqrt{2}d\overline{\alpha}_0^\circ$.

Appendix D. Determination of η_0 and η_1.

The objective of the present appendix is determining continuously differentiable functions $\eta_0 \in \mathcal{K}$ and $\eta_1 \in \mathcal{K}$ such that Eq. (52) holds.

From Eq. (49) obtain

$$|\tilde{q}(z,y,G,\tau_a)| \leq \frac{1}{\beta^*(z)}\left(\frac{1}{\tau_a}|v^*(z)| + \left|\frac{\partial v^*}{\partial z}(z)\tilde{f}_z(z,y,G)\right| + \left|\frac{\partial \beta^*}{\partial z}(z)\tilde{f}_z(z,y,G)y\right|\right) + \frac{1}{\tau_a}|y| \quad \text{(D.1)}$$

From Eq. (34) obtain $|v^*(z)| = \arcsin(|\sigma(k_p\widetilde{\Theta} + k_dQ)|) \leq \arcsin(\sigma(k_p|\widetilde{\Theta}| + k_d|Q|))$. Since $\arcsin(x) \leq 2x$ for all $0 \leq x \leq 1$ and $\sigma(x) \leq x$ for all $x \geq 0$ then

$$|v^*(z)| \leq 2(k_p|\widetilde{\Theta}| + k_d|Q|) \leq 2\sqrt{2}\ \overline{k}\|z\| \quad \text{(D.2)}$$

where $\overline{k} = \max\{k_p, k_d\}$. Moreover, the following holds

$$\left|\frac{\partial v^*}{\partial z}(z)\tilde{f}_z(z,y,G)\right| = \left|\frac{1}{\sqrt{1-\sigma^2(k_p\widetilde{\Theta} + k_dQ)}}\sigma'(k_p\widetilde{\Theta} + k_dQ)\right.$$
$$\left.(k_pQ + k_dG\sin\left(\text{sat}_{\overline{\Delta}}(v^*(z) + \beta^*(z)y)\right))\right|$$

Since $\sigma'(r) \leq 1$ for all r and $\sin(\text{sat}_{\overline{\Delta}}(x)) \leq x$ for all $x \geq 0$, it is easy to obtain the following

$$\left|\frac{\partial v^*}{\partial z}(z)\tilde{f}_z(z,y,G)\right| \leq \frac{1}{\sqrt{1-\sin^2\overline{\Delta}}}(k_p|Q| + k_dG(|v^*(z)| + \beta^*(z)|y|)$$

Thus, by using (D.2) obtain

$$\left|\frac{\partial v^*}{\partial z}(z)\tilde{f}_z(z,y,G)\right| \leq \frac{k_p + 2\sqrt{2}k_d\overline{G}\ \overline{k}}{\sqrt{1-\sin^2\overline{\Delta}}}\|z\| + \frac{k_d\overline{G}}{\sqrt{1-\sin^2\overline{\Delta}}}\beta^*(z)|y|$$
$$\forall z \in \mathbb{R}^2 \quad \forall y \in \mathbb{R} \quad \forall G \in [\underline{G}\ \overline{G}]$$

In addition

$$\left|\frac{\partial \beta^*}{\partial z}(z)\tilde{f}_z(z,y,G)\right| = \left|\frac{4}{(1+\widetilde{\Theta}^2+Q^2)^3}\left(\Theta Q + GQ\sin\left(\text{sat}_{\overline{\Delta}}(v^*(z) + \beta^*(z)y)\right)\right)y\right|$$

By using again the inequality $\sin(\text{sat}_{\overline{\Delta}}(x)) \leq x$ for all $x \geq 0$, it is easy to obtain the following

$$\left|\frac{\partial \beta^*}{\partial z}(z)\tilde{f}_z(z,y,G)\right| \leq \frac{4}{(1+\|z\|^2)^3}\left(\frac{1}{2}\|z\|^2 + \overline{G}\|z\|(|v^*(z)| + \beta^*(z)|y|)\right)|y| \qquad \forall z \in \mathbb{R}^2 \quad \forall y \in \mathbb{R} \quad \forall G \in [\underline{G}\ \overline{G}]$$

Then, by using Eq. (D.2) obtain

$$\left|\frac{\partial \beta^*}{\partial z}(z)\tilde{f}_z(z,y,G)\right| \leq \frac{4}{(1+\|z\|^2)^3}\left(\frac{1}{2} + 2\sqrt{2}\overline{Gk}\right)\|z\|^2|y| + \frac{4\overline{G}}{(1+\|z\|^2)^3}\|z\|\beta^*(z)|y| \quad \forall z \in \mathbb{R}^2 \quad \forall y \in \mathbb{R} \quad \forall G \in [\underline{G}\ \overline{G}]$$

Thus, by using the previous results, Eq. (D.1) leads to

$$|\tilde{q}(z,y,G,\tau_a)| \leq \left(\frac{2\sqrt{2}\ \overline{k}}{\underline{\tau}_a} + \frac{k_p + 2\sqrt{2}k_d\overline{Gk}}{\sqrt{1-\sin^2\overline{\Delta}}}\right)\frac{1}{\beta^*(z)}\|z\| + \left(\frac{k_d\overline{G}}{\sqrt{1-\sin^2\overline{\Delta}}} + \frac{1}{\underline{\tau}_a}\right)|y| + \frac{4}{(1+\|z\|^2)^3\beta^*(z)}\left(\frac{1}{2} + 2\sqrt{2}\overline{Gk}\right)\|z\|^2|y| + \frac{4\overline{G}}{(1+\|z\|^2)^3}\|z\||y|^2$$
$$\forall z \in \mathbb{R}^2 \quad \forall y \in \mathbb{R} \quad \forall G \in [\underline{G}\ \overline{G}] \quad \forall \tau_a \in [\underline{\tau}_a\ \overline{\tau}_a]$$

Then

$$|\tilde{q}(z,y,G,\tau_a)| \leq \left(\frac{2\sqrt{2}\ \overline{k}}{\underline{\tau}_a} + \frac{k_p + 2\sqrt{2}k_d\overline{Gk}}{\sqrt{1-\sin^2\overline{\Delta}}}\right)(\|z\| + 2\|z\|^3 + \|z\|^5) + \left(\frac{k_d\overline{G}}{\sqrt{1-\sin^2\overline{\Delta}}} + \frac{1}{\underline{\tau}_a}\right)|y| + 4\left(\frac{1}{2} + 2\sqrt{2}\overline{Gk}\right)\left(\frac{1}{2}\|z\|^4 + \frac{1}{2}|y|^2\right) + 4\overline{G}\left(\frac{1}{2}\|z\|^2 + \frac{1}{2}|y|^4\right)$$
$$\forall z \in \mathbb{R}^2 \quad \forall y \in \mathbb{R} \quad \forall G \in [\underline{G}\ \overline{G}] \quad \forall \tau_a \in [\underline{\tau}_a\ \overline{\tau}_a]$$

In conclusion, it easy to show that

$$|\tilde{q}(z,y,G,\tau_a)| \leq \eta_0(|y|) + \eta_1(\|z\|) \quad \forall z \in \mathbb{R}^2 \quad \forall y \in \mathbb{R} \quad \forall G \in [\underline{G}\ \overline{G}] \quad \forall \tau_a \in [\underline{\tau}_a\ \overline{\tau}_a]$$

with

$$\eta_0(r) = \eta_{01}r + \eta_{02}r^2 + \eta_{04}r^4 \qquad \eta_1(r) = \eta_{11}r + \eta_{12}r^2 + \eta_{13}r^3 + \eta_{14}r^4 + \eta_{15}r^5$$

where

$$\eta_{01} = \frac{k_d\overline{G}}{\sqrt{1-\sin^2\overline{\Delta}}} + \frac{1}{\underline{\tau}_a} \qquad \eta_{02} = 1 + 4\sqrt{2}\ \overline{G}\ \overline{k} \qquad \eta_{04} = 2\overline{G}$$

$$\eta_{11} = \frac{2\sqrt{2}\ \overline{k}}{\underline{\tau}_a} + \frac{k_p + 2\sqrt{2}k_d\overline{Gk}}{\sqrt{1-\sin^2\overline{\Delta}}} \quad \eta_{12} = \eta_{04} \quad \eta_{13} = 2\eta_{11} \quad \eta_{14} = \eta_{02} \quad \eta_{15} = \eta_{11}$$

Appendix E. Nomenclature

g	=	gravitational acceleration, m/s^2
I	=	moment of inertia of launch vehicle about y body axis, kg m^2
l_c	=	distance from the center of mass to engine swivel point, m
m	=	mass of launch vehicle, kg
Q	=	pitch rate, rad/s
T_c	=	control (gimbaled) thrust, N
U	=	component of velocity of center of mass along the x body axis, m/s
W	=	component of velocity of center of mass along the z body axis, m/s
Δ	=	engine deflection angle, rad
$\overline{\Delta}$	=	maximum amplitude of engine deflection angle, rad
Δ_c	=	commanded engine deflection angle, rad
τ_a	=	time constant of electro-hydraulic servoactuator, sec
Θ	=	pitch angle, rad
Θ_c	=	commanded pitch angle, rad

References

[1] A. L. Greensite, Analysis and design of space vehicle flight control systems. Control theory: Volume II, Spartan Books, New York, 1970.

[2] A. R. Mehrabian, C. Lucas, J. Roshanian, Aerospace launch vehicle control: an intelligent adaptive approach, Aerospace Science and Technology 10 (2) (2006) 149 – 155. doi:10.1016/j.ast.2005.11.002.

[3] K. Salahshoor, A. Khaki-Sedigh, P. Sarhadi, An indirect adaptive predictive control for the pitch channel autopilot of a flight system, Aerospace Science and Technology 45 (2015) 78–87. doi:10.1002/acs.2541.

[4] A. P. Nair, N. Selvaganesan, V. Lalithambika, Lyapunov based PD/PID in model reference adaptive control for satellite launch vehicle systems,

Aerospace Science and Technology 51 (2016) 70 – 77. doi:10.1016/j.ast.2016.01.017.

[5] G. Q. Xing, P. M. Bainum, F. Li, Design of a reduced order H_∞ robust controller for an expendable launch vehicle in the presence of structured and unstructured parameter uncertainty, Acta Astronautica 41 (2) (1997) 121 – 130. doi:10.1016/S0094-5765(97)00191-4.

[6] R. Das, S. Sen, S. Dasgupta, Robust and fault tolerant controller for attitude control of a satellite launch vehicle, IET Control Theory and Applications 1 (1) (2007) 304–312. doi:10.1049/iet-cta:20050518.

[7] B. Lu, D. Falde, E. Iriarte, E. Besnard, Switching robust control for a nanosatellite launch vehicle, Aerospace Science and Technology 42 (2015) 259 – 266. doi:10.1016/j.ast.2015.01.019.

[8] Y. Morita, S. Goto, Design for robustness using the μ-synthesis applied to launcher attitude and vibration control, Acta Astronautica 62 (1) (2008) 1–8. doi:10.1016/j.actaastro.2006.12.050.

[9] J. Thompson, W. O'Connor, Wave-based attitude control of spacecraft with fuel sloshing dynamics, Archive of Mechanical Engineering 63 (2) (2016) 263–275. doi:10.1515/meceng-2016-0015.

[10] U. Ansari, A. Bajodah, Robust launch vehicle's generalized dynamic inversion attitude control, Aircraft Engineering and Aerospace Technology 89 (6) (2017) 902–910. doi:10.1108/AEAT-06-2015-0149.

[11] B. Suresh, K. Sivan, Integrated Design for Space Transportation System, Springer, New Delhi, 2015.

[12] A. Tewari, Basic flight mechanics, Springer, Basel, Switzerland, 2016.

[13] A. Tewari, Advanced control of aircraft, spacecraft and rockets, Wiley, Chichester, UK, 2011.

[14] F. Tyan, D. Bernstein, Global stabilization of systems containing a double integrator using a saturated linear controller, International Journal of Robust and Nonlinear Control 9 (15) (1999) 1143–1156. doi:10.1002/(SICI)1099-1239(19991230)9:15<1143::AID-RNC455>3.0.CO;2-W.

[15] H. K. Khalil, Nonlinear systems, Prentice Hall, Upper Saddle River, NJ, 2002.

[16] P. J. Antsaklis, A. N. Michel, Linear systems, McGraw-Hill, New York, 1997.

[17] A. Isidori, Nonlinear Control Systems II, Springer Verlag, London, 1999.

[18] Y. Lin, E. D. Sontag, Y. Wang, Input to state stabilizability for parametrized families of systems, International Journal of Robust and Nonlinear Control 5 (3) (1995) 187–205. doi:10.1002/rnc.4590050304.

[19] Z. P. Jiang, A. R. Teel, L. Praly, Small-gain theorem for iss systems and applications, Mathematics of Control, Signals and Systems 7 (2) (1994) 95–120. doi:10.1007/BF01211469.

[20] H. J. Sussmann, Y. Yang, On the stabilizability of multiple integrators by means of bounded feedback controls, in: Proceedings of the IEEE Conference on Decision and Control, 1992, pp. 70–72. doi:10.1109/CDC.1991.261255.

[21] B. C. Kuo, F. Golnaraghi, Automatic control systems - 8. ed., John Wiley & Sons, 2003.